NeuroImage: Clinical 24 (2019) 101935

Contents lists available at ScienceDirect

NeuroImage: Clinical

journal homepage: www.elsevier.com/locate/ynicl

The superior longitudinal fasciculus and its functional triple-network mechanisms in brooding

D.A. Pisner[a,b,*], J. Shumake[a], C.G. Beevers[a,b], D.M. Schnyer[b]

[a] Institute for Mental Health Research (IMHR), 116 Inner Campus Dr., Austin, TX 78705, United States of America
[b] Department of Psychology, University of Texas at Austin, 108 E Dean Keeton St, Austin, TX 78712, United States of America

ARTICLE INFO

Keywords:
Multimodal
Microstructure
Resting-state
Triple-network
Brooding
Reproducibility

ABSTRACT

Brooding, which refers to a repetitive focus on one's distress, is associated with functional connectivity within Default-Mode, Salience, and Executive-Control networks (DMN; SN; ECN), comprising the so-called "triple-network" of attention. Individual differences in brain structure that might perseverate dysfunctional connectivity of brain networks associated with brooding are less clear, however. Using diffusion and functional Magnetic Resonance Imaging, we explored multimodal relationships between brooding severity, white-matter microstructure, and resting-state functional connectivity in depressed adults (N = 32–44), and then examined whether findings directly replicated in a demographically-similar, independent sample (N = 36–45). Among the fully-replicated results, three core findings emerged. First, brooding severity is associated with functional integration and segregation of the triple-network, particularly with a Precuneal subnetwork of the DMN. Second, microstructural asymmetry of the Superior Longitudinal Fasciculus (SLF) provides a robust structural connectivity basis for brooding and may account for over 20% of its severity (Discovery: adj. R^2 = 0.18; Replication: adj. R^2 = 0.22; MSE = 0.06, Predictive R^2 = 0.22). Finally, microstructure of the right SLF and auxiliary white-matter is associated with the functional connectivity correlates of brooding, both within and between components of the triple-network (Discovery: adj. R^2 = 0.21; Replication: adj. R^2 = 0.18; MSE = 0.03, Predictive R^2 = 0.21–0.22). By cross-validating multimodal discovery with replication, the present findings help to reproducibly unify disparate perspectives of brooding etiology. Based on that synthesis, our study reformulates brooding as a microstructural-functional connectivity neurophenotype.

1. Introduction

Cognitive models of depression posit that negatively biased self-referential processing plays a critical role in maintaining the disorder (Beevers, 2005). Brooding (i.e. "depressive rumination") is the *perseverative* form of this processing that involves a recursive focus on depressive thoughts to putatively gain insight that might alleviate depression symptoms (Lemoult and Joormann, 2014). In practice, however, brooding exacerbates symptoms (Lyubomirsky et al., 2015), yielding passive solutions to problems (Lyubomirsky, 2003), diminished social support (Nolen-Hoeksema and Davis, 1999), and an increased likelihood of relapse following depression treatment (Jacobs et al., 2016). Given brooding's toxic influence in depression (Woody and Gibb, 2015), both its cognitive mechanisms and developmental antecedents have been studied across multiple levels of analysis (Woody and Gibb, 2015; Bagby et al., 2004; Hankin, 2008). A deluge of recent neuroimaging studies have further propelled this effort, revealing a heterogeneous set of structural and functional brain correlates of brooding (Nejad et al., 2013) whose reproducibility and intermodal affinity remain unknown (Nolen-Hoeksema et al., 2008; Nolen-Hoeksema, 2000). The present study therefore aims to identify candidate structural-functional brain biomarkers of brooding using multimodal neuroimaging with direct replication (Woody and Gibb, 2015).

1.1. A 'triple' cognitive model and functional connectivity in brooding

Although numerous cognitive theories of brooding have been proposed (Nejad et al., 2013; Smith and Alloy, 2009), empirical evidence from functional neuroimaging has yet to definitively favor any one model over another (van Vugt and van der Velde, 2018). Common to each, however, is a tension among three core mechanisms and their associated resting-state networks (RSN's)—the latter modeled using functional Magnetic Resonance Imaging (fMRI) (Nejad et al., 2013; Wang et al., 2016; Ordaz et al., 2016; Bernstein et al., 2017). These

* Corresponding author at: 108 E Dean Keeton St, Austin, TX 78712, United States of America.
E-mail address: dpisner@utexas.edu (D.A. Pisner).

https://doi.org/10.1016/j.nicl.2019.101935
Received 2 February 2019; Received in revised form 10 July 2019; Accepted 13 July 2019
Available online 19 July 2019

include: (1) abnormal self-referential processing, which might entail poor metacognition or recursive memory recall (Leech et al., 2011; Sheline et al., 2009) as observed within the Default Mode Network (DMN); (2) negatively-biased thought appraisal, which might involve heightened discrepancy detection between self-states and goal-states (Menon and Uddin, 2010), and abnormal vigilance (Andersen et al., 2009) titration as observed within the Salience Network (SN) (Ordaz et al., 2016; Kocsel et al., 2017); and (3) impaired attentional control, which refers to top-down failures to disengage from negatively-biased self-referential processing (Southworth et al., 2017), and has been described with respect to the Executive Control Network (ECN).

With this framework as a foundation, we can use fMRI analysis to describe precise intrinsic alterations of RSN's that might relate to each respective brooding mechanism. We call this dimension of analysis *within-network* functional connectivity. One study, for instance, found that higher brooding severity is associated with alterations within a Parietal subnetwork of the DMN – the pDMN – that supports reflexive episodic memory refreshing (Rosenbaum et al., 2017; Freton et al., 2014; Ahmed et al., 2018) and is vulnerable to malfunctioning under cognitive resource depletion (Wang et al., 2016). Brooders also more actively engage a Cingulo-Opercular subnetwork of the SN – the coSN – critical for tonic alertness, as well as for maintaining ongoing emotional appraisal of internal cognitive and somatic states (Wu et al., 2016a; Sadaghiani and D'Esposito, 2015). Finally, abnormal integration of a prefrontal subnetwork of the ECN – the fECN—might reflect deficits of top-down regulation (Mandell et al., 2014) or attentional scope whereby emotionally biased information cannot be easily dispelled from working memory (Berman et al., 2011).

Other research has shown, however, that these three mechanisms and their corresponding RSN's do not operate as wholly segregated entities (Wang et al., 2016; Hamilton et al., 2015; Spreng et al., 2010; Spreng et al., 2013). Impaired attentional control, for instance, is thought to amplify and sustain negatively-biased thought appraisal (Southworth et al., 2017; Grafton et al., 2016; Koster et al., 2011). When combined with perseveration (Nolen-Hoeksema et al., 2008) and reflexive processing, this contaminated appraisal forms a vicious cycle of self-criticism (Bernstein et al., 2017; Brosschot et al., 2006) that recursively drains attentional resources needed to disengage from the processing (Southworth et al., 2016). Because these mechanisms can be mutually reinforcing at a metacognitive level, metacognitive beliefs about rumination may be particularly relevant to the etiology and treatment of brooding (Clare Kelly et al., 2008; Smith et al., 2013; Papageorgiou and Wells, 2000, 2004; Wells and Papageorgiou, 2008).

Analogously, the RSN's associated with brooding can also be described on a hierarchical basis, where the RSN's themselves are interdependent entities (Wang et al., 2016; Menon, 2011). We call this dimension of analysis *between-network* functional connectivity. As a case in point, the DMN, SN, and ECN have been described as belonging to a so-called "triple network" of attention, whose between-network connectivity may be globally compromised across depression psychopathology (Menon, 2011; Wu et al., 2016b; Liu et al., 2017; Zheng et al., 2015) (*See* Fig. 1). Using this framework, Hamilton et al. (2011) showed that the brains of brooders exhibit greater between-network DMN dominance over the ECN, with a variable role for the SN depending on level of depression severity. In another study, Wang et al. (2016) similarly argued that greater DMN dominance over the ECN, impaired SN–mediated switching between the DMN and ECN, and ineffective ECN modulation of the DMN, each constitute separate yet interactive cognitive mechanisms in brooding.

1.2. A model of individual differences and microstructural connectivity in brooding

In contrast to the cognitive process models of brooding (Smith and Alloy, 2009; Grafton et al., 2016), a complementary perspective has sought to identify its developmental antecedents. That is, "*who* becomes a ruminator" (Papageorgiou and Wells, 2004; Nolen-Hoeksema et al., 1993)? Through her longitudinal work, Nolen-Hoeksema maintained that brooding is not merely a defect of information processing, but also a Response Style (Nolen-Hoeksema et al., 1993) – i.e. an individual difference characteristic in the trait proclivity to brood (Kocsel et al., 2017; Mandell et al., 2014; Nolen-Hoeksema et al., 1993; Moore et al., 2013; Sarin et al., 2005). Although early research identified weak genetic moderators (Woody and Gibb, 2015) and environmental risk factors that may lend to brooding development as a response style (Nolen-Hoeksema et al., 2008; Papageorgiou and Wells, 2004; Watkins et al., 2005), a vigorous exploration of neurodevelopmental biomarkers is lacking. At least theoretically, such a model should include anatomical traces of grey matter thickening and white-matter myelination that implicitly encapsulate distal genetic and environmental influences, and cumulatively shape brooding into a stable trait over the lifespan (Papageorgiou and Wells, 2004).

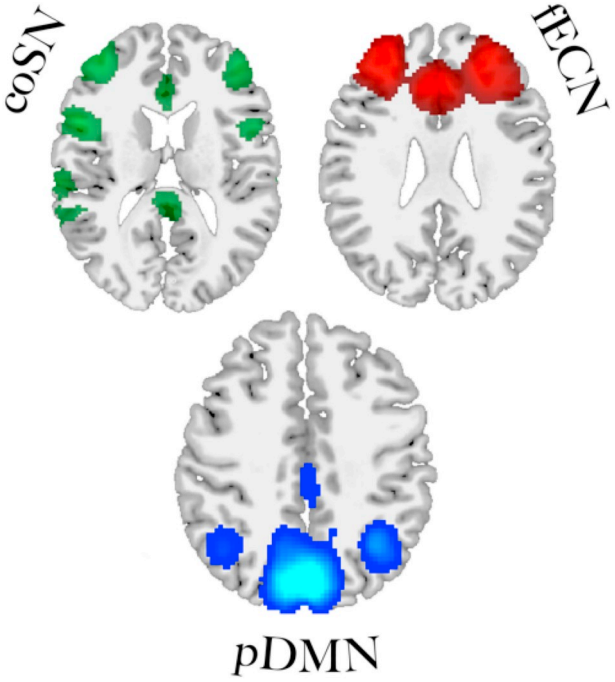

Fig. 1. The "triple-network" of attention is a mesoscale system of networks that includes the Salience Network (SN) (green), Executive Control Network (ECN) (red), and Default Mode Network (DMN) (blue), which correspond to three core mechanisms of brooding. Brooding is known to be correlated with functional connectivity disturbances both within and between these networks. (For interpretation of the references to color in this figure legend, the reader is referred to the web version of this article.)

In the search for a neurodevelopmental basis for brooding, previous structural MRI studies might provide a useful springboard (Bagby et al., 2004; Mandell et al., 2014; Kühn et al., 2012; Machino et al., 2014; Zuo et al., 2012; Fawcett et al., 2015). To the extent that resource-intensive, triple-network operations characterize a vicious cycle of negative thoughts which persist repetitively, we should likewise expect structural MRI to be sensitive to grey or white-matter biomarkers capable of scaffolding these operations over time (Nejad et al., 2013; Kühn et al., 2012; Zuo et al., 2012; Wang et al., 2015). Along these lines, some of the earliest voxel-based morphometric studies of depression looked to modular grey matter structures, like the Anterior Cingulate Cortex (ACC), whose volume, for instance, may be negatively correlated with brooding severity (Kühn et al., 2012; Machino et al., 2014; Zuo et al., 2012). Efforts to identify a straightforward role for ACC structure in brooding have been somewhat inconsistent, however (Nejad et al., 2013; Kühn et al., 2012; Cooney et al., 2010), perhaps alluding to its dense interconnectivity with other cortical areas (Etkin et al., 2011) or

the multiple specialized functions among ACC sub-regions (Stevens et al., 2011). Ultimately, appeals made to grey-matter alone have become increasingly problematic in the study of brooding because they do not reflect a commensurate level of information complexity to its functional connectivity biomarkers that verifiably exhibit distributed and dynamical neural activity (Mazzocchi, 2012; Monnart et al., 2016).

The structural analogue to functional connectivity – microstructural connectivity of white-matter (Peer et al., 2017) – may therefore provide a more flexible framework for conceptualizing individual differences in trait brooding (Woody and Gibb, 2015). Perhaps not coincidentally, BOLD signal clustering of resting-state networks produces patterns that spatially resemble white-matter tracts (Mezer et al., 2009). Like grey matter, white-matter microstructure is also highly correlated with age (Cascio et al., 2007), but due to its high plasticity distributed throughout the brain (Sampaio-Baptista and Johansen-Berg, 2017) may more closely capture the complex gene-environment diathesis that shapes myelination trajectories over the lifespan (Shi et al., 2013; Gustavson et al., 2019). Microstructural connectivity of white-matter, measured using Fractional Anisotropy (FA) (Reislev et al., 2016; Lebel and Deoni, 2018; Marstaller et al., 2016), likely track these distributed myelination patterns, which can be mapped using diffusion Magnetic Resonance Imaging (dMRI) (Yendiki et al., 2011).

Despite its potential utility for revealing neurodevelopmental vulnerabilities in depressive cognition (Korgaonkar et al., 2014; De Kwaasteniet et al., 2013; Chavez and Heatherton, 2013; Liao et al., 2013), only one study to date has explicitly investigated the microstructural basis for brooding specifically. In 2012, Zuo et al. used Tract-Based Spatial Statistics (TBSS) to show that FA of the Superior Longitudinal Fasciculus (SLF) and neighboring motor fibers are negatively associated with brooding severity. Due to its small sample size ($N = 15$) and reliance on dMRI data alone, however, that study was not strongly positioned to reconcile these microstructural connectivity correlates with known functional connectivity correlates.

1.3. A reproducible microstructural-functional connectivity model of brooding

As studies of schizophrenia have recently shown (Calhoun and Sui, 2016; Sui et al., 2014; Sui et al., 2012), multimodal analysis can uniquely fuse disparate information across modalities to formulate new ideas that encompass multiple levels of analysis simultaneously. By leveraging multimodal methodology in the study of brooding, we might discover more specific neural biomarkers, residing at the *intersection* of developmental differences and cognitive processes. Consequently, a joint analysis of rsfMRI and dMRI that seeks to reconcile patterns of functional connectivity with patterns of microstructural connectivity may prove especially informative. Perhaps through this feat, we can put Nolen-Hoeksema's Response Styles Theory to the test based on neuroscience for the first time (Calhoun and Sui, 2016; O'Halloran et al., 2016; Tadayonnejad et al., 2014; Uludağ and Roebroeck, 2014) Although recent studies beyond brooding literature have shown that frontoparietal white-matter, such as the Cingulum (CCG) and the Uncinate Fasciculus (UF), may support DMN (Tao et al., 2015) and ECN (Steffens et al., 2011) function, the precise nature of these multimodal associations remains largely unclear (Sui et al., 2012; Uludağ and Roebroeck, 2014; Pettersson-Yeo et al., 2014).

While multimodal analysis can increase sensitivity and specificity to disease biomarkers (Calhoun and Sui, 2016; Sui et al., 2012), its high dimensionality can limit the generalizability of detected effects if not balanced by additional effort towards reproducibility (Calhoun and Sui, 2016). To overcome this obstacle, without a massive sample size (Mulugeta et al., 2018), we performed out-of-sample replication within the same study (Button et al., 2013). That is, following initial analysis of a dataset collected at the University of Texas at Austin, we conducted a direct replication using an independent sample obtained from the Nathaniel Kline Institute (Nooner et al., 2012). The two samples were approximately matched on demographic criteria, contained comparable fMRI and dMRI neuroimaging data, and included nearly identical measures of brooding and depression. By exploiting this similitude, we were positioned to better evaluate the reproducibility of sufficiently-powered large effects from our Discovery sample in a Replication sample. Those findings that replicate should increase confidence in their generalizability and could be directly assessed for effect-size inflation using cross-validation (Cawley and Talbot, 2010; Evans, 2017; Poldrack et al., 2017a; Poldrack, 2019; Smith and Nichols, 2018; Nichols, 2012).

We conducted our analyses over three phrases. First, we considered unimodal microstructural and functional connectivity correlates of brooding severity so as to replicate and extend findings from prior work. To assure parallel-forms across analytic software and protect against computational error, we further analyze both rsfMRI and dMRI modalities using multiple complementary methodologies (de Haas, 2018; Bowring et al., 2018). The dMRI analyses, for instance, include dual investigations of white-matter microstructure using both Tract-Based Spatial Statistics (TBSS) and global probabilistic tractography methods (Yendiki et al., 2011). Similarly, the rsfMRI analyses include investigations of resting-state functional connectivity, using Dual-Regression (Abou Elseoud et al., 2011) and hierarchical network modeling (Parlatini et al., 2017) based on Independent Components Analysis (ICA) (Ordaz et al., 2016). For the second phase of analysis, we then assess whether the microstructural and functional connectivity biomarkers of brooding predict one another. Subsequently, we apply the same analytic pipeline used to conduct phases 1–2 of our Discovery analysis to the homogeneously preprocessed, phenotypically-similar Replication sample. Finally, we cross-validate each fully-replicated regression model to quantify mean-squared prediction error – a direct estimate of model reproducibility and alternative to the often-criticized *p*-value (Szucs and Ioannidis, 2017).

2. Methods

2.1. Participants – discovery sample

Fifty-one treatment-seeking participants with DSM-IV Major Depressive Disorder (MDD) were recruited for this study from advertisements placed online, in newspapers, and on late night TV. Participants were screened for medical or physical conditions that would preclude participation in an MRI study. They also completed an abbreviated Mini International Neuropsychiatric Interview (MINI) (Sheehan et al., 1998) to determine provisional MDD diagnosis, which were then confirmed using in-person Structured Clinical Interviews for the DSM-IV Disorders (SCID) (First et al., 1997a), and additional administration of the Beck Depressive Inventory (BDI-II) (Beck et al., 1996). Participants were further administered the RSQ (Response Styles Questionnaire) (Erdur-Bakera and Bugaya, 2010) – a 10-item self-report measure of the tendency to ruminate. To minimize brain changes associated with aging, participants were between 18 and 55 years old. Participants were excluded if they met criteria for current or past psychotic disorder, bipolar disorder, and schizophrenia. Those receiving pharmacological treatment were allowed into the study if there had been no medication change in the 12 weeks prior to study entry. Seven participants were excluded from the rsfMRI analyses (five with unusable data due to image artifact, and two for whom no rsfMRI data was acquired), yielding $N = 44$ for all unimodal rsfMRI analyses. Twelve participants were excluded from the dMRI analyses (eight for unusable data due to image artifact, and four for failed tractography reconstructions), yielding $N = 43$ and $N = 39$ for the unimodal dMRI analyses. With only one significant outlier detected across all analyses, $N = 32$ participants with both usable dMRI and rsfMRI in common remained for multimodal analyses (*See* Appendix, Methods: Section J for detailed participant accounting and quality control tracking).

2.2. Participants – replication sample

To formally test whether the findings would generalize beyond the Discovery sample (Poldrack et al., 2017b), we directly replicated all stages of analysis using a phenotypically similar, independent sample obtained from the multi-site Nathaniel Kline Institute Rockland dataset (Nooner et al., 2012). The dataset contained a sub-sample of $N = 46$ participants with similar demographics to those participants from our original sample. Participants were also between the ages of 18–55, had no severe comorbid psychopathology, had usable dMRI or rsfMRI data, reported at least some depressive symptomatology, and had been administered the 21-item Beck Depression Inventory (BDI-II) and the 22-item Rumination Response Scale (RRS)(*See* METHODS: Brooding Measurement), which contained identical brooding sub-scale items to those administered in the 10-item RSQ scale (Treynor et al., 2003). As part of a larger battery of measures, many but not all participants also completed the Structured Clinical Interview for DSM-IV-TR Axis I Disorders (SCID) (First et al., 1997b), requiring that the remaining participants be included on the basis of depressive symptomology or a history of depression diagnosis. To maximize usable data, we therefore also included dysphoric participants that had currently reported depression symptoms of > 4 (Berle and Moulds, 2013; Williams and Moulds, 2007) on the BDI-II (Beck et al., 1996). Six participants were excluded from the rsfMRI analyses (five with unusable data due to image artifact, and one which was a significant outlier across all analyses), yielding $N = 40$ for all unimodal rsfMRI analyses. Seven participants were excluded from the dMRI analyses (only one for unusable data due to image artifact, and six for failed tractography reconstructions), yielding $N = 45$ and $N = 39$ for the unimodal dMRI analyses. $N = 36$ participants with both usable dMRI and rsfMRI in common remained for multimodal analyses (*See* Appendix, Methods: Section J for detailed participant accounting and quality control tracking).

2.3. Ethics statement

For the Discovery sample, the Institutional Review Board at the University of Texas at Austin approved all study procedures and materials and all participants provided signed informed consent. For the Replication sample, Institutional Review Board approval had been previously obtained at the Nathan Kline Institute (Phase I #226781 and Phase II #239708) and at Montclair State University (Phase I #000983A and Phase II #000983B) (Nooner et al., 2012). Written informed consent was obtained for all study participants. For analysis of the Replication sample, a Data Usage Agreement (DUA) was signed and approved by all relevant parties.

2.4. Brooding measurement

The RSQ (Response Styles Questionnaire) (Erdur-Bakera and Bugaya, 2010) and the longer RRS (Rumination Response Scale) (Treynor et al., 2003) consist of a total score and two sub-scales: reflection and brooding. The reflection subscale measures an individual's tendency to engage in problem-solving whereas brooding measures the intensity of ruminative responses to expressions of negative emotion (Nolen-Hoeksema et al., 2008; Hamilton et al., 2011; Nolen-Hoeksema and Morrow, 1991). Brooding specifically reflects the intensity of ruminative responses to expressions of negative emotion (Nolen-Hoeksema and Morrow, 1991). For each item (*See* Appendix, Methods: I), participants indicate the frequency of each event on a scale ranging from 0 ("almost never") to 3 ("almost always"), yielding a range of scores from 0 to 30. The brooding subscale has high reliability ($\alpha = 0.77–0.92$) (Erdur-Bakera and Bugaya, 2010), is well-validated within depressed populations (Kühn et al., 2012), decontaminated of any explicitly depressive content (Treynor et al., 2003), and the subscale of choice for most studies of depressive rumination.

2.5. Imaging acquisition

MRI scans were acquired on a whole body 3 T GE MRI with an 8-channel phase array head coil. The scanning protocol involved collection of a localizer followed by a high-resolution T1 structural scan, two resting state scans of 6 min each, a second high-resolution structural scan, and finally a 55-direction diffusion MRI (dMRI) scan. Since not all participants had both resting-state scans, only the first of the two was analyzed by default, unless visual inspection revealed overt artifact in which case the second scan was used if it was available. For the resting-state scan, instructions were presented utilizing a back-projection screen located in the MR bore and viewed through a mirror mounted on the head coil. Participants were instructed to remain awake and alert and keep their gaze on a fixation cross (+) presented approximately at the center of their field of view for the duration of the scan. (*See* Appendix, Methods: Section A).

2.6. dMRI: Preprocessing

Preprocessing of dMRI data was carried out using a custom workflow that included eddy correction, brain extraction, denoising, and tensor/ball-and-stick model fitting tools adapted from the FMRIB Diffusion Toolbox (Jenkinson et al., 2012). To achieve maximal sensitivity and specificity from the dMRI data, preprocessing included rigorous automated and manual quality control steps (*See* Appendix, Methods: B).

2.7. dMRI: tract-based spatial statistics (TBSS) and global probabilistic tractography

A number of approaches to dMRI analysis were implemented. To begin, the whole-brain data was interrogated using Tract-Based Spatial Statistics (TBSS) (Smith et al., 2006) to identify microstructural characteristics that were associated with brooding severity (*See* Appendix, Methods: Section C). We additionally employed the 'crossing-fibers' extension of TBSS (Jbabdi et al., 2010), which allowed for greater specificity than TBSS based on the tensor model alone, because it is sensitive to the impact of cross-fibers. For statistical testing, a permutation approach was employed using FSL's "randomise" function with the TFCE Threshold-Free Cluster Enhancement option, generating 10,000 permutations and applying family-wise error (FWE)-correction to obtain cluster inferences. A two-tailed regression model was next generated using FSL's GLM function, whereby RSQ brooding scores were used as the criterion variable with age and gender as nuisance covariates. Age was included to control for typical white matter changes that would occur across the aging spectrum (Westlye et al., 2010), and gender was included due to known brain differences based on sex (Kaiser et al., 2009; Inano et al., 2011), along with some evidence of gender differences in brooding—namely, that females tend to be more severe ruminators than males (Nolen-Hoeksema, 1987).

Following TBSS, we sought to corroborate our initial group level, voxel-wise dMRI findings using individual-level tractography, which is an alternative dMRI analysis methodology that attempts to reconstruct known white-matter pathways while retaining each subject's image in native space orientation. Because spatial information is not manipulated in tractography as it is with TBSS (De Groot et al., 2013), tractography could confirm any TBSS findings as reflecting actual underlying white-matter differences rather than differences introduced during the image normalization process (Torgerson et al., 2013). For tractography, we chose to define microstructure as average weighted FA measures from the entire pathways of tracts of interest whose labels included > 5 significant voxels from the earlier TBSS stage. These measures were then further analyzed across hemispheres to establish any significant laterality effects (Vernooij et al., 2007). To perform tractography, we specifically used the TRActs Constrained by UnderLying Anatomy (TRACULA) tool in FreeSurfer (version 5.3.0) (Yendiki

et al., 2011), which delineates 18 known white-matter bundles in a fully-automated, unbiased manner using each participant's joint dMRI and T1-weighted MRI reconstruction (*See* Appendix, Methods: Section D). Because this process involves joint reconstructions, it can often fail to reconstruct all tracts successfully, even after reinitialization, if both the T1-weighted and dMRI images do not closely conform to those used in the default 'training-set.' Thus, tractography was performed on most, but not all participants (*See* Appendix, Methods: Section J).

2.8. rsfMRI preprocessing

Preprocessing of baseline rsfMRI data was carried out using FSL's FEAT (Jenkinson et al., 2012), combined with AFNI and FREESURFER tools. Additional control for white-matter and ventricular Cerebral-Spinal Fluid confounds was included, and denoising was carried out using FSL's ICA-based Xnoisifier artifact removal tool (FIX) to control for motion and physiological artifact based on an unbiased classifier (*See* Appendix, Methods: Section E).

2.9. rsfMRI: dual-regression and hierarchical network modeling

Group-level Independent Components Analysis (ICA) was performed by employing "temporal concatenation" of the complete, preprocessed rsfMRI time-series from all of the participants and restricted to twenty-five independent component (IC) outputs (Beckmann, 2009). Four IC's were manually identified as noise and removed from further examination. Of the remaining twenty-one networks, all were identified using visual inspection by way of reference to the 17 RSN's delineated by the Yeo et al. 2011 atlas (Thomas Yeo et al., 2011), thus allowing for identification of the three IC's of the triple-network established from prior work – the pDMN (Rosenbaum et al., 2017; Hamilton et al., 2011), the coSN (Wu et al., 2016b), and the fECN (Bernstein et al., 2017; Dutta et al., 2014).

A dual-regression approach (Smith, 2012) was next performed on the triple-network RSN's, which were used as regressors for each participant's rsfMRI dataset in order to extract time-series that were both specific to each participant and to each of the three IC's (Cascio et al., 2007). Design matrices and contrasts were then created to test for correlations between brooding severity and total average intrinsic connectivity within each of these RSN's, controlling for age and gender. These regression models were tested separately for each RSN, using two-tailed contrasts in an identical manner to that used in TBSS, with FSL's randomise (10,000 permutations) and TFCE cluster-thresholding with whole-brain FWE-correction (Smith and Nichols, 2009). To further correct for analysis-level multiple comparisons among the three triple-network RSN's, we also Bonferroni-corrected our alpha significance level for these models to 0.05/3 or $p = .0167$.

To investigate interactions between the triple-network RSN's, we used FSLNets (Smith et al., 2013), a MATLAB-based tool that interfaces with FSL. FSLNets treats the group-ICA outputs (generated from the earlier dual-regression stage) as RSN nodes for hierarchical network modeling. This involved estimating a partial-correlation matrix of the triple-network RSN's for each participant. To perform between-RSN general linear modeling, randomise (Berle and Moulds, 2013) was again employed with FWE-correction, but this time using the nets_glm function with 10,000 permutations. The design matrices and contrasts used in the earlier FSL GLM analyses, were used in this analysis as well.

2.10. Cross-validating discovery

To minimize potentially confounding sample-variant effects due to incongruence of neuroimaging acquisition parameters across samples (Gouttard et al., 2008), we spatially and temporally resampled the rsfMRI and dMRI data in the Replication sample to match that of the Discovery sample (*See* Appendix, Methods: Sections F & G). To ensure direct equivalence of neuroimaging data preprocessing in the replication (Bowring et al., 2018), we also applied an equivalent analytic pipeline to that applied to the discovery sample, but using the pDMN, fECN, and coSN RSN definitions from the Discovery sample group-ICA as the input to both dual-regression and FSLnets. Lastly, given the multiple scanner sites used to collect the neuroimaging data in the Replication sample, we employed mixed-effects regression models (both with FSL's GLM and in R 3.4.0), whereby a scanner-site factor was additionally modeled as a random effect. Thus, we report conditional $R^{2'}$ (cond. $R^{2'}$) values for Replication sample regression analyses, where effect sizes are contingent upon the influence of scanner site.

To ensure adequate power to justify replication based on the Discovery findings, we conducted power analyses for detecting a large effect size when using multiple regression with two covariates (age and gender) (Kocsel et al., 2017; Treynor et al., 2003; Butler and Nolen-Hoeksema, 1994) (*See* Appendix: Methods, Section H). To decrease the risk of false-discovery made in the Discovery sample, we also opted to filter significant effects by a minimum cutoff of unadjusted $R^2 = 0.25$ and $p < .01$ FDR for non-voxel-wise tests (i.e. tractography, multimodal analysis of beta-coefficients) and whole-brain $p < .05$ FWE-corrected threshold for voxel-wise tests (TBSS, Dual-Regression). This step served to more stringently identify those findings with the greatest practical significance, highest putative generalizability, and lowest risk of replication failure. Further, we conservatively classified a finding as being a 'full replication' if it replicated with respect to both directionality of the effect, the RSN's or neuroanatomical label(s) implicated, and its laterality. Likewise, the fully-replicated findings needed to meet our effect-size cutoff in at least one of the two samples and survive a Family-Wise Error (FWE)/False Discovery Rate (FDR)-corrected significance level of $\alpha < 0.05$ (Eklund et al., 2016) or $\alpha < 0.001$ uncorrected for ROI analyses (Poldrack and Mumford, 2009). To directly quantify predictive test error, we used each regression model to predict the corresponding dependent variable from the Replication sample based on a 4-fold cross-validation, where the four scanner sites of the Replication sample could be conveniently used as 'natural' fold assignments to avoid the need for mixed modeling in out-of-sample prediction. We then calculated the mean squared error (MSE) between the values predicted by the Discovery sample and the actual outcome values from the Replication sample. This out-of-sample error could then be used to derive a predictive R (Lemoult and Joormann, 2014), which is the proportion of variance in the Replication sample that is explained by the model fit to the Discovery sample (Alexander et al., 2015; Fox, 2019). That is to say, for each Replication sample outcome value $y_i \in R$, $\forall\, i = 1, 2, \ldots, n$ where $\hat{y}$ is the predicted value based on the Discovery sample estimator, we define MSE and R^2 as $MSE(y, \hat{y}) = \frac{1}{n}\sum_{i=1}^{n}(y_i - \hat{y})^2$ and $R^2(y, \hat{y}) = 1 - \frac{\sum_{i=1}^{n}(y_i - \hat{y})^2}{\sum_{i=1}^{n}(y_i - \bar{y})^2}$, respectively. That predictive R^2 could then be compared to the fit R^2 values from the corresponding Discovery-sample estimator to infer the extent of optimistic bias in the within-sample estimates of effect size.

3. Results

3.1. Demographic, behavioral, and clinical characteristics

3.1.1. Discovery sample

Brooding severity as measured using the RSQ was normally distributed ($M = 9.06$, $SD = 3.44$, range: 1–15, IQR = 5; Shapiro-Wilk = 0.971, $p = .24$). Depression severity was also normally distributed ($M = 31.98$, $SD = 8.16$, range: 17–48, IQR = 10, Shapiro-Wilk = 0.975, $p = .35$) and was modestly associated with brooding severity (adj. $R^2 = 0.11$, $F(1, 49) = 7.11$, $p < .05$). Age was positively skewed ($M = 28.71$, $SD = 9.76$, range: 18–56) due to an over-representation of young adults in our discovery sample. There was an approximately even gender distribution (females = 29). Whereas 18% of Discovery sample participants had not experienced a past depressive

Table 1
The table compares key characteristics of both Discovery and Replication samples.

Sample characteristics	Discovery sample	Replication sample
Age	*M* = 28.71, *SD* = 9.76, Range: 18–56	*M* = 31.02, *SD* = 6.07, Range: 22–45
Gender	29 females (57%)	31 females (67%)
Brooding Severity	*M* = 9.06, *SD* = 3.44	*M* = 10.91, *SD* = 2.86
Depression Diagnosis	Current depression only, DSM-IV diagnosed	Current or past depression, DSM-IV diagnosed or BDI-II symptomatic
Depressive Episodes	82% Reported > 1 past episodes	38% Reported > 1 past episodes
Depression Severity	*Moderate-severe* BDI-II: *M* = 31.98, *SD* = 8.16	*Dysphoric-Severe* BDI-II: *M* = 10.39, *SD* = 7.08
Medication Useage	Excluded if medication changes reported within 12 weeks prior to study entry	Excluded if medication change data available
Other Psychopathology	26% current, 51% past comorbidity	28% current, 56% past comorbidity
Scanner Type	Siemens Skyra 3 T	Siemens Tim Trio 3 T
Multi-site?	No	Yes, 4 separate sites
dMRI parameters	TR/TE = 1200/71.1, B = 1000, 128 × 128 matrix, 3 mm slice thickness, anistropic voxels, 2 B0 + 53 DWI (55-directions)	TR/TE = 2400/85, B = 1500, 212 × 212 matrix, 2 mm slice thickness, isotropic voxels, 9 B0 + 128 DWI (137-directions)
rsfMRI parameters	eyes open, TR = 2000 ms, TE = 30 ms, 31 axial slices, voxel size = 3.125 × 3.125 × 3 mm^3 anisotropic	eyes open, TR = 2000 ms, TE = 30 ms, 40 axial slices, voxel size = 3 × 3 × 3 mm^3 isotropic

episode, 82% had reported one or more prior episodes. Additionally, 28% of participants reported currently having comorbid symptoms of one or more non-exclusionary disorders (*See* METHODS: Participants – *Discovery Sample*). Participant exclusion on the basis of neuroimaging artifact and modality subsampling did not significantly alter demographic makeup. No significant correlations were detected between brooding severity and age or gender in either Discovery or Replication samples. Nevertheless, we retained both age and gender as nuisance covariates for each regression model to control for their established interactions with neuroimaging measures, previously identified relationships with brooding and depression severity from other studies, as well as to ensure maximal generalizability and consistency across our analyses and samples.

3.1.2. Replication sample

The Replication sample exhibited similar descriptive statistics to those of the Discovery sample (*See* Table 1**)**. Average brooding severity was similar across samples (*M* = 10.91, *SD* = 2.86, range: 6–20, IQR = 3) with marginal but non-significant positive skew (Shapiro-Wilk = 0.952, *p* = .06). Age also exhibited a marginal positive skew (*M* = 31.02, *SD* = 6.07, Range: 22–45; Shapiro-Wilk = 0.953, *p* = .06) as it did in the Discovery sample. Unlike in the Discovery sample, however, the Replication sample was less gender balanced (females = 31). Furthermore, 62% of the participants had never experienced a past depressive episode, and only 38% had reported at least one prior episode. With the less stringent dysphoria inclusion criterion, depression severity was also notably lower in the Replication sample (*M* = 10.39, *SD* = 7.08, range: 4–34, IQR = 5). Nevertheless, comorbidity profiles were similar to those of the Discovery sample. 51% of Replication sample participants reported having experienced symptoms of one or more non-depressive disorders and 26% of participants reported currently having comorbid symptoms of one or more non-exclusionary disorders (*See* METHODS: Participants – *Replication Sample*). Participant exclusion on the basis of neuroimaging artifact and modality subsampling again did not significantly alter demographic makeup. Detailed participant comorbidity characteristics of the Discovery and Replication samples can be found in Tables I and II of the Appendix, Results: Section A. When applying the analytic methdology used for our Discovery sample to the Replication sample (*See* METHODS: Replication), we directly cross-validated the Discovery findings across each level of analysis—1) triple-network functional connectivity and brooding; 2) microstructural connectivity and brooding; 3) microstructural-functional connectivity and brooding. Cross-validation involved testing the Discovery sample regression models directly on the Replication sample, and then reporting MSE as a measure of the out-of-sample prediction error. Ultimately, the *derived* values of Predictive R^2 were similar to the *estimated* values and did not demonstrate any signs of systematic inflation so long as the R^2 estimates were adjusted for degrees of freedom. Thus, we opted to report only the adjusted (and predictive) R^2 effect sizes for all model estimation results.

3.2. 'Within-network' functional connectivity and depressive brooding

In both samples, brooding was associated with resting-state functional connectivity of the three triple-network RSN's as identified from the outputs of group-ICA followed by dual-regression (METHODS: rsfMRI Group-ICA & Dual-regression). More precisely, brooding was correlated with functional connectivity in multiple clusters belonging to

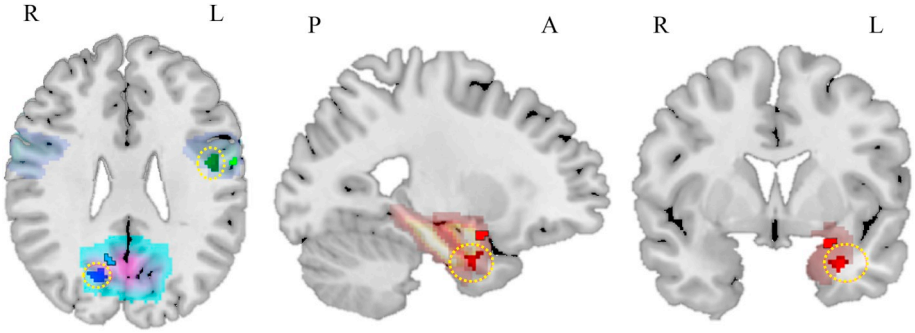

Fig. 2. Replicated within-network functional connectivity findings from the Replication sample are indicated with dark shaded red, green, and blue clusters along with surrounding dotted yellow ovals, as compared to lighter-shaded clusters from the Discovery sample. In both samples, Blue clusters depict those areas of the right Precuneus with significantly lower functional connectivity within the pDMN in association with brooding. Green clusters depict those areas of the left Precentral Gyrus with significantly lower functional connectivity of the coSN in association with brooding. Red clusters depict those areas of the left Amygdala and Parahippocampal Gyrus with greater functional connectivity within the fECN in association with brooding. (For interpretation of the references to color in this figure legend, the reader is referred to the web version of this article.)

each respective triple-network RSN (i.e. 'intrinsic' connectivity), but also to others that were outside of the respective RSN's (i.e. 'extrinsic' connectivity) (*see* Fig. 2). With respect to intrinsic connectivity, brooding was associated with lower functional connectivity of the pDMN with the right Precuneus (MSE = 0.04, Predictive $R^2 = 0.34$; Discovery: $p < .01$ FWE; Replication: $p < .001$ with a minimum distance of 4.5 voxels between significant clusters across samples (*see blue clusters in* Fig. 2). With respect to extrinsic connectivity, brooding was positively associated with functional connectivity of the frontal Executive Control Network (fECN) and the inferior Temporal Lobe between the left Amygdala and Parahippocampal Gyrus (MSE = 0.05, Predictive $R^2 = 0.12$; Discovery: $p < .05$ FWE; Replication: $p < .001$ with a minimum distance of 9.7 voxels between significant clusters across samples) (*See red clusters in* Fig. 2). Lastly, the Cingulo-Opercular Salience Network (coSN) exhibited lower intrinsic functional connectivity in the left dorsal Precentral Gyrus near Broca's area (Discovery: $p < .01$ FWE; Replication: $p < .001$ with a minimum distance of 1 voxel between significant clusters across samples) (*See green clusters in* Fig. 2). With a very strong effect (Predictive $R^2 = 0.63$), but comparatively high prediction error (MSE = 0.10), this coSN-brooding model was only significant in the Replication sample when controlling both for depression severity ($p < .01$) and a gender-coSN interaction ($p < .05$). The gender term was needed due to a gender imbalance in the Replication sample and because gender is a known moderator of the SN in relation to brooding (Ordaz et al., 2016).

3.3. 'Between-network' functional connectivity and depressive brooding

Based on prior evidence for the role of the pDMN, coSN, and fECN in brooding, we next used FSLnets to explore whether between-network functional connectivity of each pair combination of triple-network RSN's correlated with brooding severity (*see* METHODS: Between-Network Functional Connectivity). FSLnets revealed that brooding severity was positively associated with an inverse correlation between the fECN and pDMN in both samples (MSE = 0.04, Predictive $R^2 = 0.26$; Discovery: $p < .05$ FDR; Replication: $p < .05$, FDR) (*See* Fig. 3). Although an inverse correlation was also detected between the coSN and the pDMN in the Discovery sample ($p < .01$ FDR), this effect only marginally replicated ($p < .06$ FDR), and required controlling for the gender-coSN interaction and depression severity. The third 'between-network' correlation (fECN-coSN) was not significantly associated with brooding in either the Discovery or Replication samples.

3.4. Microstructural connectivity and brooding

3.4.1. Tract-based spatial statistics (TBSS)

Our next set of analyses sought to identify any microstructural associations with brooding. To achieve this, we first employed TBSS (*see* METHODS: TBSS; Appendix, Methods: Section C). In first exploring a neurodevelopmental basis for these associations, we observed a robust negative correlation with age across samples ($F(1,37) = 4.58$, adj. $R^2 = 0.11$, $p < .05$; $F(1,37) = 4.85$, adj. $R^2 = 0.08$, $p < .05$). In association with higher brooding severity, our results first revealed significantly lower FA within several large clusters covering the right Superior Longitudinal Fasciculus (SLF, parietal and temporal parts), as well as within smaller clusters of the Cingulum, right posterior Corpus Callosum (i.e. Splenium), and Corticospinal Tract (CST) (MSE = 0.04, Predictive $R^2 = 0.10$; Discovery: $p < .01$ FWE; Replication: $p < .05$ FWE). At the $p = .05$ FWE threshold in TBSS, 98 voxels, located in the SLF, CST, and Corpus Callosum overlapped across samples, and covered a key posterior section of right SLF-Splenium fibers adjacent to the right Precuneus (*See zones of convergence demarcated in green in* Fig. 4). Some of these clusters also extended into the Anterior Thalamic Radiation (ATR), Uncinate Fasciculus (UF), and Splenium. In general, however, it was the right SLF-T specifically that most prominently drove the effect in both samples.

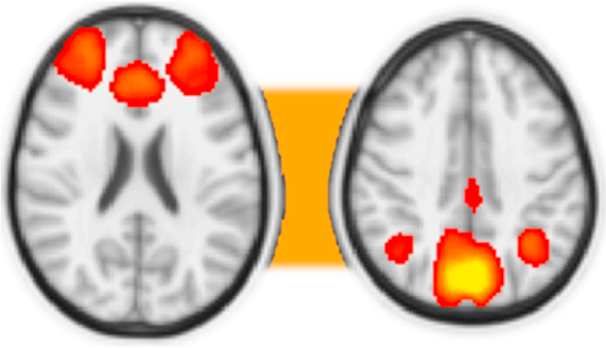

Fig. 3. The image depicts the fECN (*left*) and pDMN (*right*) whose inverse correlation was associated with brooding severity. (For interpretation of the references to color in this figure legend, the reader is referred to the web version of this article.)

3.4.2. Global probabilistic tractography

Although TBSS is sensitive to whole-brain white-matter associations, tractography offers greater specificity for labeling known white-matter pathways (Yendiki et al., 2011; De Groot et al., 2013). Because it can be performed in native diffusion space, it is therefore largely immune from artifact that might result from the geometric transformations involved in the normalization step in TBSS. Hence, we employed tractography alongside TBSS to ensure the reliability of the TBSS findings and gain greater location specificity. Towards that end, six pathways of interest were automatically parcellated with tractography and included the SLF, CCG, CST, ATR, UF, and Splenium. As also indicated from the TBSS analysis, tractography revealed a negative correlation between weighted average FA of the right SLF-T and brooding severity in both samples at Bonferroni-corrected thresholds (MSE = 0.06, Predictive $R^2 = 0.22$; Discovery: adj. $R^2 = 0.18$, $F(3, 36) = 3.85$, $p_{corrected} < 0.005$; Replication: adj. Cond. $R^2 = 0.22$, $F(3, 35) = 8.90$, $p_{corrected} < 0.005$).

3.4.3. Tract hemisphericity

Both TBSS and tractography analyses indicated that the SLF-T finding was distinctly right-lateralized. To test this formally, we treated hemisphere as a within-subjects measure and used Analysis of Variance (ANOVA) to compare two GLM's predicting brooding for each tractography measure of global average FA. Specifically, the first GLM used left hemisphere controlling for right hemisphere as the predictor, whereas the second used right hemisphere controlling for left hemisphere. On the basis of log-likelihood, we found supportive evidence for right lateralization of the SLF-T in its association with brooding in both samples (Discovery: $F(2,36) = 8.71$, $p < .005$; Replication: $F(2,36) = 5.43$, $p < .05$).

3.5. Multimodal connectivity (microstructural-functional) and brooding

3.5.1. Microstructure supports 'within-network' functional connectivity in brooding

To explore any multimodal relationships between the microstructural and the functional connectivity findings, we next extracted the beta coefficients representing average total intrinsic connectivity for each of the brooding-associated triple-network clusters discovered through dual-regression. This involved creating a matched subsample of $N = 32$ in the Discovery sample and $N = 36$ in the Replication sample to be used for all multimodal analyses, since those participants with unusable dMRI data were not the same as those with unusable fMRI data (*See* Appendix, Methods: Section J). As an initial step, we extracted beta-coefficients of within-network functional connectivity disruptions in brooding for each participant, and then regressed these coefficients against whole-brain white-matter on an FWE-corrected

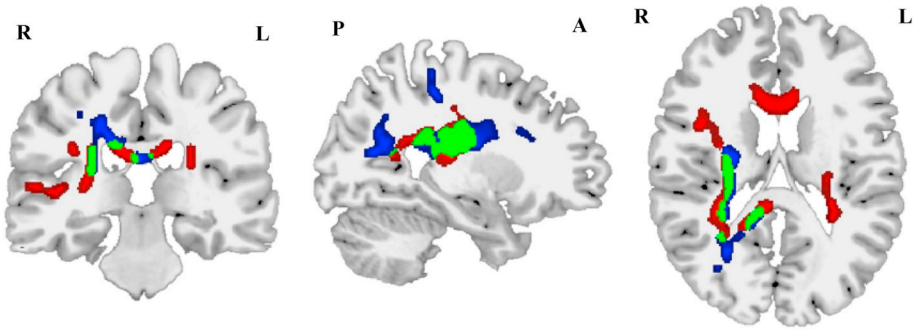

Fig. 4. The mosaic depicts TBSS negative correlations with brooding revealed from the Discovery sample ($p = .01$ FWE; blue) and the Replication sample ($p = .05$ FWE; red). These findings overlapped closely (green) along the right SLF and along the Splenium of the Corpus Callosum. (For interpretation of the references to color in this figure legend, the reader is referred to the web version of this article.)

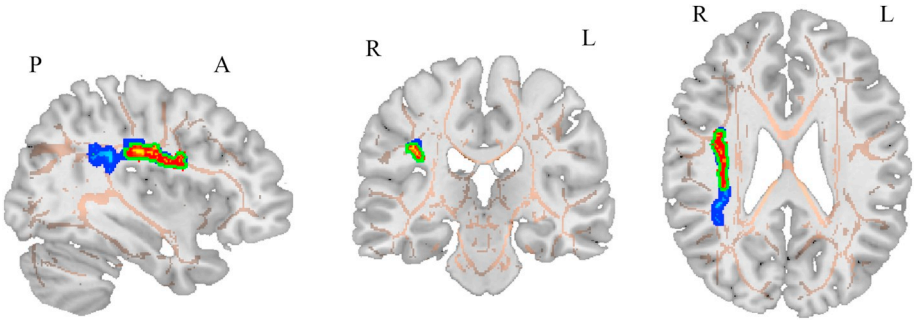

Fig. 5. The slices depict a positive correlation between functional the diminished within-network functional connectivity of the pDMN associated with brooding and the right SLF, as discovered using TBSS. The Discovery sample ($p = .05$ FWE) is again depicted in blue, whereas the Replication sample ($p = .001$) is depicted in red. These findings overlapped closely (shown in green outline) along the right SLF-T. (For interpretation of the references to color in this figure legend, the reader is referred to the web version of this article.)

voxel-wise basis using TBSS. Results showed that pDMN within-network functional connectivity disruptions in brooding were positively associated with microstructure of the right SLF-T in both samples (MSE = 0.03, Predictive $R^2 = 0.24$; Discovery: $p < .05$ FWE; Replication: $p < .05$ FWE). 613 voxels along the white matter skeleton overlapped across samples and were predominantly restricted to the temporal part of the right SLF (*See* Fig. 5). Our tractography measures of the right SLF-T and SLFP further substantiated these findings, again revealing a robust positive association between the SLF-T and the pDMN within-network functional connectivity clusters associated with brooding (MSE = 0.03, Predictive $R^2 = 0.22$; Discovery: adj. $R^2 = 0.21$, $F(3, 29) = 3.59$, $p < .05$; Replication: adj. Cond. $R^2 = 0.18$, $p < .05$). Stepwise regression revealed that the best model, where right SLF-T microstructure interacts with both the pDMN and fECN individually, could predict over 40% of the variance in brooding with minimal error (Predictive $R^2 = 0.42$, MSE = 0.03).

3.5.2. Microstructure supports 'between-network' functional connectivity in brooding

We next tested whether microstructural associates of brooding were correlated with the *between-network* functional connectivity disruptions of the triple-network in brooding. Although the tractography measure of the right SLF-T was not significantly associated with between-network functional connectivity when using FA values in FSLnets, average FA of the cumulative set of brooding-associated clusters identified from TBSS (i.e. ATR, CST, CCG, Splenium, UF, and SLF) ($p = .05$ FWE) was positively associated with pDMN-fECN between-network functional connectivity (Discovery: $p < .05$ FDR; Replication: $p < .05$ FDR). Although Predictive $R^2 = 0.39$ was strong for this association, error was high (MSE = 0.08), perhaps indicating that *linear* models may fail to capture the association with optimal generalization.

4. Summary

In sum, both samples revealed: (1) brooding severity was associated with triple-network intrinsic and extrinsic functional connectivity alterations; (2) brooding severity was also associated with auxiliary clusters of CCG, CST, ATR, Splenium, and UF white-matter, but most prominently with the SLF-T (i.e. the Arcuate Fasciculus), which we found to consistently explain over 20% of the variance in brooding across samples; (3) the right SLF-T was further multimodally associated with pDMN within-network functional connectivity alterations in brooding; (4) cumulative brooding-associated microstructural differences were correlated with pDMN-fECN between-network functional dysconnectivity in brooding. See Fig. 6 for a visual summary of findings from all levels of analysis and Table 2 for a comparison of key findings across Discovery and Replication samples.

5. Discussion

The aim of the present study was to evaluate a multimodal neural connectivity basis for brooding that might in turn help to clarify its apparently multifactorial etiology. Towards that end, results converged across multiple levels of analysis and directly replicated across two independent samples, revealing at least seven distinct candidate biomarkers of brooding, two of which were multimodal. Apart from differences in depression severity and gender makeup, Discovery and Replication samples were matched on key behavioral characteristics: both comprised of predominantly young adults with equivalent measures of brooding, similar inclusion criteria, and comparable neuroimaging acquisition parameters. Using a combination of exploratory regression analysis and cross-validation, our results first showed that brooding is associated with various patterns of functional disorganization among a trio of resting-state subnetworks—the Precuneal Default Mode (pDMN), the Cingulo-Opercular Salience (SN), and the frontal Executive Control (fECN) networks (Thomas Yeo et al., 2011). Building upon prior work (Wang et al., 2016; Hamilton et al., 2015; Spreng et al., 2010; Spreng et al., 2013; Hamilton et al., 2011), this initial set of findings served to isolate key components of these networks, and their patterns of interaction, that may support a hierarchical system of neurocognitive mechanisms in brooding. Second, our findings showed that microstructure of the right Superior Longitudinal Fasciculus (SLF) can distinguish among varying levels of brooding severity. In unifying these dimensions of analysis, we then demonstrate that brooding-associated functional connectivity alterations of the pDMN (both its within- and between-network profiles) are associated with white-matter dysconnectivity of the right SLF-T. Ultimately, our findings support the notion that the interface of right SLF-T microstructural connectivity and

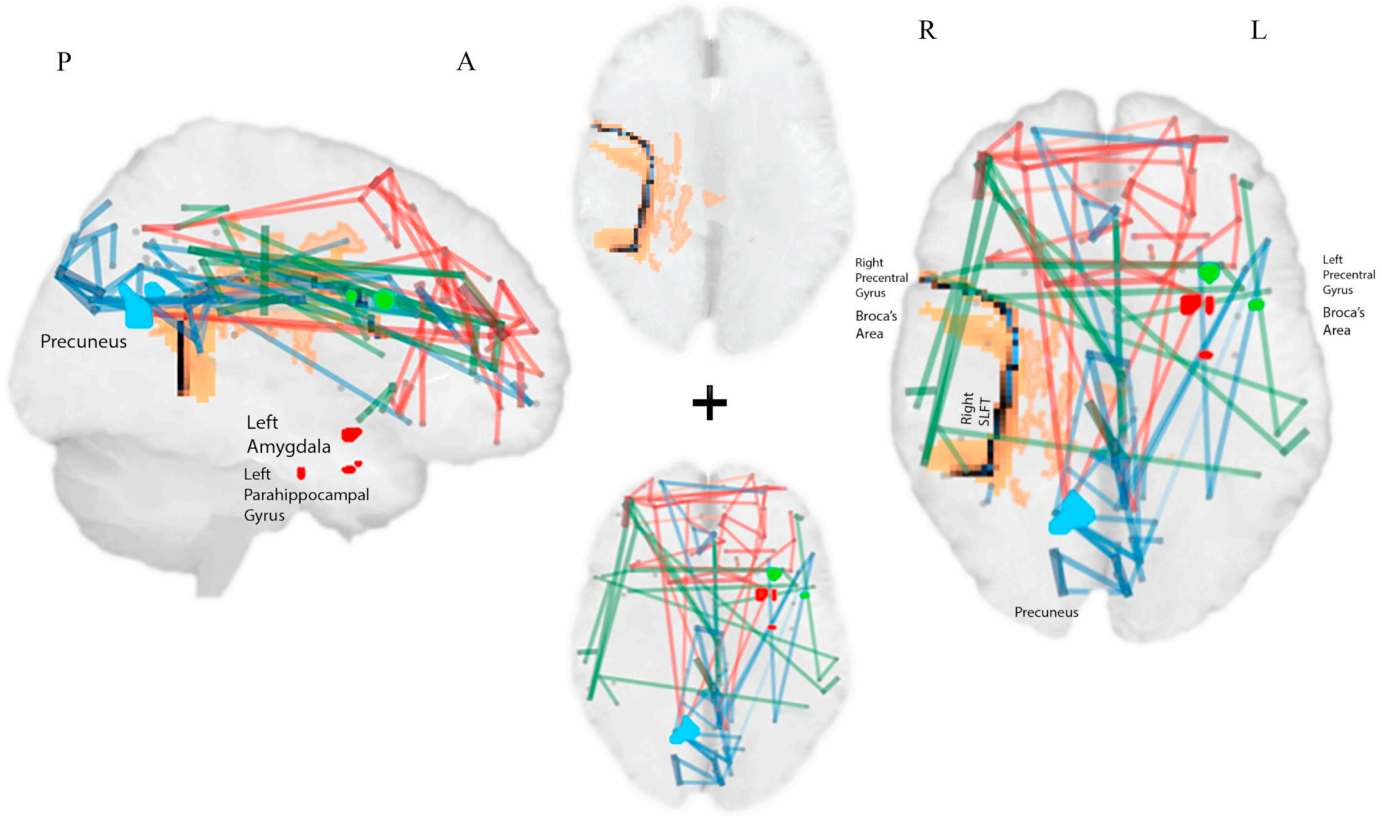

Fig. 6. The visualization summarizes the replicated microstructural and functional connectivity findings, depicted both independently (center slices) and multimodally (outside slices), with brooding across samples. Microstructural correlates of brooding including the right SLF-T and auxiliary pathways revealed from TBSS and tractography are represented in copper-black heatmap. Each of the pDMN, coSN, and fECN as a whole are here depicted as distinct yet clearly overlapping networks with blue, green, and red connections, respectively. Regions whose functional connectivity within the pDMN are disrupted in brooding are depicted in blue blobs, whereas those of the coSN and fECN are depicted in green and red blobs, respectively. (For interpretation of the references to color in this figure legend, the reader is referred to the web version of this article.)

triple-network functional connectivity captures a crucial and previously unknown feature that supports brooding in depression (Woody and Gibb, 2015; Sarin et al., 2005; Scott, 2009; Schmaling et al., 2002; Hilt et al., 2012).

5.1. A triple-network functional connectivity model of brooding

Among the fully-replicated results, we observed several defining functional connectivity features associated with brooding. The first of these was lower functional connectivity of the right Precuneus within the pDMN—a finding that has also been observed in studies of memory (Züst et al., 2015; Klaassens et al., 2017) and in the context of the

Table 2
The table depicts seven key findings (*left column*) that directly and fully replicated across the discovery sample (*second column*) and replication sample (*third column*), along with Mean-Square Error (MSE) and Predictive R^2 values revealed through cross-validation across samples (*fourth column*). Each of the second and third columns states the R^2 value from the respective regression models (adjusted in the Discovery sample, adjusted and conditional on random effects in the Replication sample), the methodology used to estimate that value (e.g. TBSS, tractography, dual-regression, FSLnets), and the directionality of the relationship (*neg = negative, pos = positive*).

Regression Findings (Predictor and Outcome)	Initial Sample	Replication Sample	Meta-Analysis
Right SLFT Microstructure and Brooding Severity	Tractography (adj. $R^2 = 0.18$, neg)	Tractography (adj. Cond. $R^2 = 0.22$, neg)	MSE = 0.06 Predictive $R^2 = 0.22$
Distributed CST, UF, SLF, CCG, and Splenium Microstructure and Brooding Severity	TBSS ($p < .01$ FWE, neg)	TBSS ($p < .01$ FWE, neg)	MSE = 0.04 Predictive $R^2 = 0.10$
pDMN Within-Network Connectivity and Brooding Severity	Dual-regression ($p < .01$, FWE, neg)	Dual-regression ($p < .001$, neg)	MSE = 0.03 Predictive $R^2 = 0.34$
fECN Within-Network Connectivity and Brooding Severity	Dual-regression ($p < .01$, FWE, neg)	Dual-regression ($p < .001$, neg)	MSE = 0.05 Predictive $R^2 = 0.12$
pDMN-fECN Between-Network Connectivity and Brooding Severity	FSLnets ($p < .05$, FDR, neg)	FSLnets ($p < .01$, FDR, neg)	MSE = 0.04 Predictive $R^2 = 0.26$
Right SLFT Microstructure and Brooding-Associated pDMN Within-Network Connectivity	Tract. (adj. $R^2 = 0.21$, $p < .05$, pos) TBSS ($p < .05$ FWE, pos)	Tract. (adj. Cond. $R^2 = 0.18$, $p < .05$, pos) TBSS ($p < .05$ FWE, pos)	MSE = 0.03 Predictive $R^2 = 0.22$–0.24
Distributed CST, UF, SLF, CCG, and Splenium Microstructure and pDMN-fECN Between-Network Connectivity	FSLnets ($p < .05$ FDR, pos)	FSLnets ($p < .05$ FDR, pos)	MSE = 0.08 Predictive $R^2 = 0.39$

disorganized thinking of Schizophrenia (Utevsky et al., 2014; Wang et al., 2017). Our functional connectivity analyses also indicated that brooding is associated with alterations of the coSN, particularly with respect to clusters of the left Precentral Gyrus and Broca's Area. Mirroring observations from other studies of the coSN in rumination (Ordaz et al., 2016; Hamilton et al., 2011), however, this effect was confounded by gender and depression severity, both of which varied across samples, and will therefore require larger, heterogeneous sample sizes to confirm. More cogently, we discovered greater fECN-Parahippocampal connectivity in association with higher brooding severity in both samples, echoing similar connectivity patterns to those sometimes observed in abnormal context suppression (Phelps and Sharot, 2008). Adjacently, brooding severity was positively associated with fECN within-network connectivity of the left Amygdala. This heightened fronto-limbic integration would appear to reflect a core faulty belief in brooding – namely, that recursive replay of depressive thoughts affords practical insights that can help to alleviate depression symptoms (Lemoult and Joormann, 2014). Protecting this belief in brooding's usefulness (Cohen et al., 2016; Watkins and Brown, 2002), albeit perhaps counterintuitive, would seem to require some form of repeated suppression, both of the emotional discomfort elicited by the depressive thoughts themselves and the real-life contexts upon which those are based. Sustained top-down control via the fECN may well support such mechanisms.

Relatedly, brooding severity was negatively associated with a between-network inverse correlation of the pDMN and fECN across samples. That relationship reiterates a well-established pattern of asynchrony between self-referential and cognitive control systems as a defining feature of brooding (Wang et al., 2016; Spreng et al., 2010; Hamilton et al., 2011). Our study extends that understanding, however, by considering abnormal pDMN-fECN segregation against the backdrop of the replicated within-network pDMN-Precuneal dysconnectivity and fECN-limbic connectivity findings as well. Collectively, these findings would appear to support the Impaired Disengagement Hypothesis (Grafton et al., 2016; Koster et al., 2011) of brooding, which holds that the processing of self-referent material becomes elaborative (i.e. ruminative) when attentional faculties fail to disengage from the negative aspects of that material. Correspondingly, reflexive pDMN processing may become elaborative when the fECN fails to disengage from the negatively salient features of that processing, perhaps in part due to poor vigilance titration by the coSN. By this framework, brooding would seem to entail both independent *and* overlapping neurocognitive mechanisms of impaired disengagement, recruiting both intrinsic and extrinsic properties of the triple-network RSN's. This need not imply exclusivity of these RSN's alone in brooding – other networks may be relevant; what *is* clear is that this hierarchical system is distinctly reproducible across various brain models of brooding (Ordaz et al., 2016; Rosenbaum et al., 2017; Hamilton et al., 2015; Zheng et al., 2015; Hamilton et al., 2011; Dutta et al., 2014; Menon, 2011).

5.2. A microstructural connectivity model of brooding

Studying connectivity dynamics of the triple-network can illuminate functional processes that characterize brooding and allow for hypothesis formulation with respect to component cognitive mechanisms. An exclusive focus on patterns of brain function, however, fails to explain why these mechanisms exhibit trait-like persistence over time, and why they become pathological for some, but not all, brains (Nolen-Hoeksema and Davis, 1999; Nolen-Hoeksema et al., 1993). To explore a possible neuroanatomical basis for the trait dimension of brooding – what Nolen-Hoeksema once called a 'Response Style' – we next investigated its microstructural correlates using dMRI. Those results revealed robust associations with the Superior Longitudinal Fasciculus, along with additional clusters scattered throughout the Cingulum, Corticospinal Tract, Splenium, Uncinate Fasciculus, Anterior Thalamic Radiation, and Corona Radiata. Although these white-matter correlates cumulatively replicated across samples, tractography revealed that the microstructure of one global white-matter pathway in particular – the temporal part of the Superior Longitudinal Fasciculus (SLF-T) – could explain over 20% of the variance in brooding severity on average across samples. Not only did this biomarker replicate at Bonferroni-corrected thresholds across samples, it did so with consistent right-dominant hemisphere asymmetry.

By employing both tractography and TBSS methodologies in tandem (Urgerl et al., 2013), moreover, we were also well-positioned to explore specific subdivisions of the SLF that were most closely associated with brooding (Makris et al., 2005). Using tractography, for instance, we learned that brooding was globally associated with a portion of the SLF connecting the middle/superior Temporal Gyrus with ipsilateral Precentral/Cingulo-Opercular areas. This SLF-T subdivision, also known as the Arcuate Fasciculus, supplies bidirectional connections throughout temporal, parietal, and frontal lobes. Although it is a bilateral association tract, the SLF-T of the dominant hemisphere also critically connects Wernicke's area for speech production and Broca's area for language comprehension. Given its highly specialized functional neuroanatomy, dysconnectivity of the SLF-T in the context of brooding could be associated with abnormal language and memory systems in the brain, and specifically those responsible for maintaining ongoing phonological awareness (Jenkins et al., 2016; Oechslin et al., 2009). Research on the microstructural basis of conduction aphasia has shown, for instance, that differences in SLF-T microstructure may be related to disrupted awareness of speech repetition (Bernal and Ardila, 2009). In fact, stutterers exhibit lower integrity of the SLFT relative to non-stutterers (Cieslak et al., 2015). As TBSS also indicated, the most prominent SLF-T disturbance was in a medial-temporal/inferior-frontal cluster of white-matter that may be particularly relevant for the circulation of words and speech sounds in the service of short-term memory (Baldo et al., 2012). Future work should therefore explore whether these microstructural abnormalities of the SLF-T are specifically associated with repetitive, perseverative thinking and recall in brooding.

Across both samples, microstructural connectivity of the right SLF was also significantly lower in females relative to males, and negatively correlated with age. Hence, SLF *asymmetry* may be a critical neurodevelopmental biomarker of brooding (Shi et al., 2013; Westlye et al., 2010; Agarwal et al., 2016; Klingberg et al., 1999; Ugwu et al., 2014), albeit future longitudinal dMRI studies will be needed to confirm this. Still, abnormal cerebral lateralization has been hypothesized as far back as Martin's 1989 Goal-Progress Theory of brooding (Martin and Tesser, 1989; Martin et al., 2008) even though this has never been shown using measures of white-matter microstructure specifically. In both of our samples, the asymmetry was distinctly right-lateralized, which might lend to several interpretations grounded in theories of cerebral specialization (Gazzaniga, 2000). For instance, cortical areas connected by the right SLF-T, such as the right temporoparietal junction and right superior temporal gyrus, have been implicated in monological speech (Geva et al., 2011; Alderson-Day and Fernyhough, 2015) and may exhibit grey-matter differences in brooding (Machino et al., 2014). Studies of Schizophrenia have likewise reported SLF-T asymmetry in association with auditory hallucinations and disorganized speech (De Weijer et al., 2011). Conversely, greater connectivity of the left SLF-T has been observed in the brains of long-term meditators who are presumably trained to 'suspend' ruminative thinking (Luders et al., 2011). In sum, SLF-T asymmetry is a key white-matter biomarker of brooding that may reflect atypical patterns of language development critical for monological speech repetition and phonological short-term memory.

5.3. A microstructural-functional connectivity model of brooding

Although the triple-network functional connectivity model of brooding may provide insight into *how* brooding unfolds (i.e. through dysregulated, negatively-biased self-referential processing), it does not offer an account of *why* it occurs recursively or persists as a stable trait.

By exploring functional connectivity correlates (a neuromechanistic perspective) alongside structural connectivity correlates (a neurodevelopmental perspective), and then fusing those investigations together using simple regression models with multimodal features, we were thereby positioned to begin testing these overarching questions more directly. Our multimodal analysis accordingly revealed that microstructure of the right SLF-T was moderately associated with pDMN within-network functional connectivity in both samples. Hence, recursive self-referential processing in brooding may be largely maintained by asymmetric development of phonological memory and language repetition via the SLF-T, but additional studies will be needed to confirm this. Beyond the SLF, the cumulative influence of distributed microstructural associates of brooding were further weakly correlated with the between-network pDMN-fECN inverse correlation in both samples. This finding clarifies that candidate mechanisms of brooding like impaired-disengagement may be at least partially trait-sustained.

Based on these multimodal findings, we posit that functional triple-network disorganization, together with microstructural inefficiency of the SLF and auxiliary white-matter, captures a duplexity of brain features with mutual relevance to the etiology of brooding. The neurodevelopmental evolution of this microstructural-functional connectivity phenotype remains largely unclear, however. Nevertheless, we might appeal to theories like the "perseverative cognition hypothesis" (Brosschot et al., 2006) which holds that perseverative cognitive processes like brooding lead to a prolonged stress response—a systemic change that may alter myelination patterns in both developing and mature brains (Nugent et al., 2015; Sheikh et al., 2014). To the extent that the perseverative cognition of brooding involves repetitive cognitive processing that may accompany stress response, irregular myelination trajectories might accumulate in brooding-associated pathways to support the added cognitive load. In fact, recent evidence has shown that chronic stress in depression can systematically disrupt axon-myelin adhesion in specific pathways like the Corpus Callosum by suppressing metabotropic glutamate receptor activation in oligodendrocytes (Miyata et al., 2016). Still, a precise understanding of how distributed brain structure and function evolve together in the context of brooding will be the work of future longitudinal studies.

5.4. Limitations and generalizability

By validating our findings with a replication sample, our study contributes the first verifiably generalizable brain model of brooding to the larger corpus of depression literature (Evans, 2017; Eklund et al., 2016). We interpret the relative success of our replication attempt as indicative that under conditions of sufficient sample uniformity, neuroimaging analysis can detect reproducible patterns of brain structure and function associated with brooding severity. Although suboptimal sample sizes may be susceptible to effect-size inflation (Eklund et al., 2016; Cremers et al., 2017), our study further demonstrates that predictive test-error can be used to directly measure the extent of that inflation (Szucs and Ioannidis, 2017). Above all, we demonstrate how direct replication with open-datasets can serve as a powerful, data-economic (de Haas, 2018) tool for cross-validating scientific discovery.

One limitation of the present study may be that the candidate neural biomarkers that it uncovered are not purely attributable to brooding. Given the high co-occurrence of brooding with depression, however, there are fundamental obstacles to establishing specificity of brooding biomarkers to depression (Beck et al., 1996). Although some specificity can be assumed (Smith and Alloy, 2009), there is an unavoidable restricted range of brooding *extent* (i.e. severity) among non-depressed individuals (Bagby et al., 2004; Roelofs et al., 2006). Nevertheless, participants included in our more heterogeneous Replication sample exhibited a variety of dysphoric and/or depression backgrounds, thereby enabling us to at least broadly infer that the replicated neural correlates of brooding are reproducibly observable across a relatively heterogeneous depressive sample.

6. Conclusion

In the present study, we aimed to both identify and unify candidate biomarkers of brooding, which we achieved in the form of seven fully-replicated microstructural and functional connectivity correlates that were cross-validated across two independent samples. Results from both datasets first supported a functional network model of brooding; that is, brooding severity is associated with disorganized patterns of resting-state functional connectivity of the 'triple-network' consisting of subnetworks of the DMN, SN, and ECN. These networks have both intrinsic and extrinsic connectivity properties that may underlie a triple-cognitive process model of brooding mechanisms— recursive self-referential processing, negatively-biased thought appraisal, and impaired attentional disengagement. Converging across multiple methods of analysis applied to both datasets, our results showed that individual differences in Superior Longitudinal Fasciculus and auxiliary white-matter microstructure may largely account for the severity of trait brooding. Finally, the discovery of multimodal associations between microstructural and functional connectivity correlates of brooding provides a fresh avenue for reconciling cognitive process models with trait developmental models. Most centrally, individuals with asymmetrical development of language pathways may be uniquely prone to the biased, recursive, self-referential processing that would seem to largely define brooding.

By cross-validating multimodal discovery with out-of-sample prediction, our study leverages reproducibility as a tool for testing broader theories of brooding, such as a fusion of etiological perspectives in the spirit of Nolen-Hoeksema's Response Styles Theory (Nolen-Hoeksema et al., 1993). Our hope is that the findings presented will help to accelerate neuroscientific understanding of a key maintaining factor in depression, perhaps easing our own brooding as clinical scientists in the process. Equipped with the certitude that such knowledge can provide, we might in turn refine the individualized depression treatments of tomorrow—based on multimodal brain biomarkers whose reproducibility is *known*.

Author contributions

Derek Pisner conceived of the study and discussed it with David Schnyer and Christopher Beevers, who obtained the funding and supervised the data collection for the discovery sample. Derek Pisner obtained the replication sample from the Nathaniel Kline Institute. Derek Pisner conducted all the analyses and processed the neuroimaging data with the help of research assistants. Jason Shumake provided consultation on the choice of statistical analyses. Derek Pisner wrote the manuscript and all co-authors provided critical feedback throughout the writing process. All authors approved the final manuscript.

Acknowledgements

The research reported in this publication was supported by the National Institute of Mental Health of the National Institutes of Health under awards R21MH092430 and R33MH109600. The content is solely the responsibility of the authors and does not necessarily represent the official views of the National Institutes of Health. We would first like to thank the technical staff at the Texas Advanced Computing Center for supplying the computational resources that would have otherwise rendered our neuroimaging analyses computationally intractable. We would also like to thank Ryan Hammonds for assistance with data quality control. Finally, we would also like to thank Ari Cohen for her incredible patience and support throughout the drafting of this manuscript.

Appendix A. Supplementary data

Supplementary data to this article can be found online at https://

doi.org/10.1016/j.nicl.2019.101935.

References

Abou Elseoud, A., et al., 2011. Group-ICA model order highlights patterns of functional brain connectivity. Front. Syst. Neurosci. 5 (37).

Agarwal, S., Stamatakis, E.A., Geva, S., Warburton, E.A., 2016. Dominant hemisphere functional networks compensate for structural connectivity loss to preserve phonological retrieval with aging. Brain Behav 6 (1–14).

Ahmed, S., et al., 2018. Association between precuneus volume and autobiographical memory impairment in posterior cortical atrophy: beyond the visual syndrome. NeuroImage Clin. 18, 822–834.

Alderson-Day, B., Fernyhough, C., 2015. Inner speech: development, cognitive functions, phenomenology, and neurobiology. Psychol. Bull. 141, 931–965.

Alexander, D.L.J., Tropsha, A., Winkler, D.A., 2015. Beware of R^2: simple, unambiguous assessment of the prediction accuracy of QSAR and QSPR models. J. Chem. Inf. Model. 55 (7), 1316–1322.

Andersen, S.B., Moore, R.A., Venables, L., Corr, P.J., 2009. Electrophysiological correlates of anxious rumination. Int. J. Psychophysiol. 71, 156–169.

Bagby, R.M., Rector, N.A., Bacchiochi, J.R., McBride, C., 2004. The stability of the response styles questionnaire rumination scale in a sample of patients with major depression. Cogn. Ther. Res. 28, 527–538.

Baldo, J.V., Katseff, S., Dronkers, N.F., 2012. Brain regions underlying repetition and auditory-verbal short-term memory deficits in aphasia: evidence from voxel-based lesion symptom mapping. Aphasiology 26 (3-4), 338–354.

Beck, A., Steer, R., Brown, G., 1996. Beck Depression Inventory-II. San Antonio. pp. 12–15.

Beckmann, Mackay, 2009. Filippini & Smith. Group comparison of resting-state FMRI data using multi-subject ICA and dual regression. Neuroimage 47 (S148).

Beevers, C.G., 2005. Cognitive vulnerability to depression: a dual process model. Clin. Psychol. Rev. 25, 975–1002.

Berle, D., Moulds, M.L., 2013. Emotional reasoning processes and dysphoric mood: cross-sectional and prospective relationships. PLoS One 8 (6), e67359.

Berman, M.G., et al., 2011. Neural and behavioral effects of interference resolution in depression and rumination. Cogn. Affect. Behav. Neurosci. 11 (1), 85–96.

Bernal, B., Ardila, A., 2009. The role of the arcuate fasciculus in conduction aphasia. Brain 132, 2309–2316.

Bernstein, E.E., Heeren, A., McNally, R.J., 2017. Unpacking rumination and executive control: a network perspective. Clin. Psychol. Sci. 5 (5), 816–826.

Bowring, A., Maumet, C., Nichols, T., 2018. Exploring the impact of analysis software on task fMRI results. bioRxiv 40 (11), 3362–3384.

Brosschot, J.F., Gerin, W., Thayer, J.F., 2006. The perseverative cognition hypothesis: a review of worry, prolonged stress-related physiological activation, and health. J. Psychosom. Res. 60 (2), 113–124.

Butler, L.D., Nolen-Hoeksema, S., 1994. Gender differences in responses to depressed mood in a college sample. Sex Roles 30, 331–346.

Button, K.S., et al., 2013. Power failure: why small sample size undermines the reliability of neuroscience. Nat. Rev. Neurosci. 14, 365–376.

Calhoun, V.D., Sui, J., 2016. Multimodal fusion of brain imaging data: a key to finding the missing link(s) in complex mental illness. Biol. Psychiatry Cogn. Neurosci. Neuroimaging 1 (3), 230–244.

Cascio, C.J., Gerig, G., Piven, J., 2007. Diffusion tensor imaging: application to the study of the developing brain. J. Am. Acad. Child Adolesc. Psychiatry 46, 213–223.

Cawley, G.C., Talbot, N.L.C., 2010. On over-fitting in model selection and subsequent selection bias in performance evaluation. J. Mach. Learn. Res. 11, 2079–2107.

Chavez, R.S., Heatherton, T.F., 2013. Multimodal frontostriatal connectivity underlies individual differences in self-esteem. Soc. Cogn. Affect. Neurosci. 10 (3), 364–370.

Cieslak, M., Ingham, R.J., Ingham, J.C., Grafton, S.T., 2015. Anomalous white matter morphology in adults who stutter. J. Speech Lang. Hear. Res. 58 (2), 268–277.

Clare Kelly, A.M., Uddin, L.Q., Biswal, B.B., Castellanos, F.X., Milham, M.P., 2008. Competition between functional brain networks mediates behavioral variability. Neuroimage 39, 527–537.

Cohen, N., et al., 2016. Using executive control training to suppress amygdala reactivity to aversive information. Neuroimage 125, 1022–1031.

Cooney, R.E., Joormann, J., Eugène, F., Dennis, E.L., Gotlib, I.H., 2010. Neural correlates of rumination in depression. Cogn. Affect. Behav. Neurosci. 10, 470–478.

Cremers, H.R., Wager, T.D., Yarkoni, T., 2017. The relation between statistical power and inference in fMRI. PLoS One 12 (1–21).

De Groot, M., et al., 2013. Improving alignment in tract-based spatial statistics: evaluation and optimization of image registration. Neuroimage 76, 400–411.

de Haas, B., 2018. How to enhance the power to detect brain-behavior correlations with limited resources. Front. Hum. Neurosci. 12 (421).

De Kwaasteniet, B., et al., 2013. Relation between structural and functional connectivity in major depressive disorder. Biol. Psychiatry 74, 40–47.

De Weijer, A.D., et al., 2011. Microstructural alterations of the arcuate fasciculus in schizophrenia patients with frequent auditory verbal hallucinations. Schizophr. Res. 130 (1-3), 68–77.

Dutta, A., McKie, S., Deakin, J.F.W., 2014. Resting state networks in major depressive disorder. Psychiatry Res. 224, 139–151.

Eklund, A., Nichols, T.E., Knutsson, H., 2016. Cluster failure: why fMRI inferences for spatial extent have inflated false-positive rates. Proc. Natl. Acad. Sci. 113 (28), 7900–7905.

Erdur-Bakera, Ö., Bugaya, A., 2010. The short version of ruminative response scale: reliability, validity and its relation to psychological symptoms. Proc. – Soc. Behav. Sci. 5, 2178–2181.

Etkin, A., Egner, T., Kalisch, R., 2011. Emotional processing in anterior cingulate and medial prefrontal. Trends Cogn. Sci. 15, 85–93.

Evans, S., 2017. What has replication ever done for us? Insights from neuroimaging of speech perception. Front. Hum. Neurosci. 11, 41 eCollection.

Fawcett, J.M., et al., 2015. The origins of repetitive thought in rumination: separating cognitive style from deficits in inhibitory control over memory. J. Behav. Ther. Exp. Psychiatry 47, 1–8.

First, M.B., Spitzer, R.L., Gibbon, M., Williams, J.B.W., 1997a. Structured Clinical Interview for DSM-IV Axis I Disorders, Clinician Version (SCID-CV) for DSMIV.

First, M.B., Gibbon, M., Spitzer, R.L., Gibbon, M., Williams, J.B.W., 1997b. Structured Clinical Interview for DSM-IV Axis II Personality Disorders (SCID-II). American Psychiatric Press, Inc.

Fox, D.G., 2019. Judging Air Quality Model Performance. pp. 8–11.

Freton, M., et al., 2014. The eye of the self: precuneus volume and visual perspective during autobiographical memory retrieval. Brain Struct. Funct. 219 (3), 959–968.

Gazzaniga, M.S., 2000. Cerebral specialization and interhemispheric communication: does the corpus callosum enable the human condition? Brain 123 (7), 1293–1326.

Geva, S., et al., 2011. The neural correlates of inner speech defined by voxel-based lesion-symptom mapping. Brain 134, 3071–3082.

Gouttard, S., Styner, M., Prastawa, M., Piven, J. & Gerig, G. Assessment of reliability of multi-site neuroimaging via traveling phantom study. In Lecture Notes in Computer Science (including subseries Lecture Notes in Artificial Intelligence and Lecture Notes in Bioinformatics) (2008).

Grafton, B., Southworth, F., Watkins, E.R., MacLeod, C., 2016. Stuck in a sad place: biased attentional disengagement in rumination. Emotion 16, 63–72.

Gustavson, D.E., et al., 2019. Predominantly global genetic influences on individual white matter tract microstructure. Neuroimage 184, 871–880.

Hamilton, J.P., et al., 2011. Default-mode and task-positive network activity in major depressive disorder: implications for adaptive and maladaptive rumination. Biol. Psychiatry 70, 327–333.

Hamilton, J.P., Farmer, M., Fogelman, P., Gotlib, I.H., 2015. Depressive rumination, the default-mode network, and the dark matter of clinical neuroscience. Biol. Psychiatry 78, 224–230.

Hankin, B.L., 2008. Stability of cognitive vulnerabilities to depression: a short-term prospective multiwave study. J. Abnorm. Psychol. 117 (2), 324–333.

Hilt, L.M., Armstrong, J.M., Essex, M.J., 2012. Early family context and development of adolescent ruminative style: moderation by temperament. Cognit. Emot. 26 (5), 916–926.

Inano, S., Takao, H., Hayashi, N., Abe, O., Ohtomo, K., 2011. Effects of age and gender on white matter integrity. Am. J. Neuroradiol. 32, 2103–2109.

Jacobs, R.H., et al., 2016. Targeting ruminative thinking in adolescents at risk for depressive relapse: rumination-focused cognitive behavior therapy in a pilot randomized controlled trial with resting state fMRI. PLoS One 11.

Jbabdi, S., Behrens, T.E.J., Smith, S.M., 2010. Crossing fibres in tract-based spatial statistics. Neuroimage 49, 249–256.

Jenkins, L.M., et al., 2016. Shared white matter alterations across emotional disorders: a voxel-based meta-analysis of fractional anisotropy. NeuroImage Clin. 12, 1022–1034.

Jenkinson, M., Beckmann, C.F., Behrens, T.E.J., Woolrich, M.W., Smith, S.M., 2012. FSL. NeuroImage 62, 782–790.

Kaiser, A., Haller, S., Schmitz, S., Nitsch, C., 2009. On sex/gender related similarities and differences in fMRI language research. Brain Res. Rev. 61, 49–59.

Klaassens, B.L., et al., 2017. Diminished posterior precuneus connectivity with the default mode network differentiates normal aging from Alzheimer's disease. Front. Aging Neurosci. 9 (97).

Klingberg, T., Vaidya, C.J., Gabrieli, J.D., Moseley, M.E., Hedehus, M., 1999. Myelination and organization of the frontal white matter in children: a diffusion tensor MRI study. Neuroreport 10, 2817–2821.

Kocsel, N., et al., 2017. Trait rumination influences neural correlates of the anticipation but not the consumption phase of reward processing. Front. Behav. Neurosci. 11.

Korgaonkar, M.S., Fornito, A., Williams, L.M., Grieve, S.M., 2014. Abnormal structural networks characterize major depressive disorder: a connectome analysis. Biol. Psychiatry 76, 567–574.

Koster, E.H.W., De Lissnyder, E., Derakshan, N., De Raedt, R., 2011. Understanding depressive rumination from a cognitive science perspective: the impaired disengagement hypothesis. Clin. Psychol. Rev. 31, 138–145.

Kühn, S., Vanderhasselt, M.A., De Raedt, R., Gallinat, J., 2012. Why ruminators won't stop: the structural and resting state correlates of rumination and its relation to depression. J. Affect. Disord. 141, 352–360.

Lebel, C., Deoni, S., 2018. The development of brain white matter microstructure. Neuroimage 182, 207–218.

Leech, R., Kamourieh, S., Beckmann, C.F., Sharp, D.J., 2011. Fractionating the default mode network: distinct contributions of the ventral and dorsal posterior cingulate cortex to cognitive control. J. Neurosci. 31, 3217–3224.

Lemoult, J., Joormann, J., 2014. Depressive rumination alters cortisol decline in major depressive disorder. Biol. Psychol. 100, 50–55.

Liao, Y., et al., 2013. Is depression a disconnection syndrome? Meta- analysis of diffusion tensor imaging studies in patients with MDD. J. Psychiatry Neurosci. 38, 49–56.

Liu, Y., et al., 2017. Decreased triple network connectivity in patients with recent onset post-traumatic stress disorder after a single prolonged trauma exposure. Sci. Rep. 7.

Luders, E., Clark, K., Narr, K.L., Toga, A.W., 2011. Neuroimage 57, 1308–1316.

Lyubomirsky, S. The consequences of dysphoric rumination. In Rumination: Nature, Theory, and Treatment of Negative Thinking in Depression (2003).

Lyubomirsky, S., Layous, K., Bay, E., Chancellor, J., Nelson-coffey, S.K., 2015. Thinking About Rumination: The Scholarly Contributions and Intellectual Legacy of Susan Nolen-Hoeksema.

Machino, A., et al., 2014. Possible involvement of rumination in gray matter

abnormalities in persistent symptoms of major depression: an exploratory magnetic resonance imaging voxel-based morphometry study. J. Affect. Disord. 168, 229–235.
Makris, N., et al., 2005. Segmentation of subcomponents within the superior longitudinal fascicle in humans: a quantitative, in vivo, DT-MRI study. Cereb. Cortex 15, 854–869.
Mandell, D., Siegle, G.J., Shutt, L., Feldmiller, J., Thase, M.E., 2014. Neural substrates of trait ruminations in depression. J. Abnorm. Psychol. 123, 35–48.
Marstaller, L., Burianová, H., Reutens, D.C., 2016. Individual differences in structural and functional connectivity predict speed of emotion discrimination. Cortex 85, 65–74.
Martin, L.L., Tesser, A., 1989. Toward a motivational and structural theory of ruminative thought. In: Unintended Thought.
Martin, L.L., Shrira, I., Startup, H.M., 2008. Rumination as a function of goal progress, stop rules, and cerebral lateralization. In: Depressive Rumination: Nature, Theory and Treatment.
Mazzocchi, F., 2012. Complexity and the reductionism-holism debate in systems biology. Wiley Interdiscip. Rev. Syst. Biol. Med. 4 (5), 413–427.
Menon, V., 2011. Large-scale brain networks and psychopathology: a unifying triple network model. Trends Cogn. Sci. 15, 483–506.
Menon, V., Uddin, L.Q., 2010. Saliency, switching, attention and control: a network model of insula function. Brain Struct. Funct. 214, 655–667.
Mezer, A., Yovel, Y., Pasternak, O., Gorfine, T., Assaf, Y., 2009. Cluster analysis of resting-state fMRI time series. Neuroimage 45 (4), 1117–1125.
Miyata, S., et al., 2016. Association between chronic stress-induced structural abnormalities in Ranvier nodes and reduced oligodendrocyte activity in major depression. Sci. Rep. 6, 23084.
Monnart, A., Kornreich, C., Verbanck, P., Campanella, S., 2016. Just swap out of negative vibes? Rumination and inhibition deficits in major depressive disorder: data from event-related potentials studies. Front. Psychol. 7.
Moore, M.N., et al., 2013. Genetic and environmental influences on rumination, distraction, and depressed mood in adolescence. Clin. Psychol. Sci. 1, 316–322.
Mulugeta, L., et al., 2018. Credibility, replicability, and reproducibility in simulation for biomedicine and clinical applications in neuroscience credibility in simulation for. Biomed. Clin. Appl. 12, 1–16.
Nejad, A.B., Fossati, P., Lemogne, C., 2013. Self-referential processing, rumination, and cortical midline structures in major depression. Front. Hum. Neurosci. 7 (666).
Nichols, T.E., 2012. Multiple testing corrections, nonparametric methods, and random field theory. Neuroimage 62, 811–815.
Nolen-Hoeksema, S., 1987. Sex differences in unipolar depression: evidence and theory. Psychol. Bull. 101, 259–282.
Nolen-Hoeksema, S., 2000. The role of rumination in depressive disorders and mixed anxiety/depressive symptoms. J. Abnorm. Psychol. 109, 504–511.
Nolen-Hoeksema, S., Davis, C.G., 1999. 'Thanks for sharing that': ruminators and their social support networks. J. Pers. Soc. Psychol. 77 (4), 801–814.
Nolen-Hoeksema, S., Morrow, J., 1991. A prospective study of depression and posttraumatic stress symptoms after a natural disaster: the 1989 Loma Prieta earthquake. J. Pers. Soc. Psychol. 61, 115–121.
Nolen-Hoeksema, S., Morrow, J., Fredrickson, B.L., 1993. Response styles and the duration of episodes of depressed mood. J. Abnorm. Psychol. 102, 20–28.
Nolen-Hoeksema, S., Wisco, B.E., Lyubomirsky, S., 2008. Rethinking rumination. Perspect. Psychol. Sci. 3, 400–424.
Nooner, K.B., et al., 2012. The NKI-Rockland sample: a model for accelerating the pace of discovery science in psychiatry. Front. Neurosci. 6, 152 eCollection.
Nugent, K.L., et al., 2015. Cortisol reactivity to stress and its association with white matter integrity in adults with schizophrenia. Psychosom. Med. 77 (7), 733–742.
Oechslin, M.S., Imfeld, A., Loenneker, T., Meyer, M., Jäncke, L., 2009. The plasticity of the superior longitudinal fasciculus as a function of musical expertise: a diffusion tensor imaging study. Front. Hum. Neurosci. 3, 76.
O'Halloran, R., Kopell, B.H., Sprooten, E., Goodman, W.K., Frangou, S., 2016. Multimodal neuroimaging-informed clinical applications in neuropsychiatric disorders. Front. Psychiatry 7 (1–14).
Ordaz, S.J., et al., 2016. Ruminative brooding is associated with salience network coherence in early pubertal youth. *Soc. Cogn. Affect. Neurosci.* nsw133.
Papageorgiou, C., Wells, A., 2000. Treatment of recurrent major depression with attention training. Cogn. Behav. Pract. 7, 407–413.
Papageorgiou, Costas, Wells, A., 2004. Depressive Rumination: Nature, Theory and Treatment. John Wiley & Sons, Ltd.
Parlatini, V., et al., 2017. Functional segregation and integration within fronto-parietal networks. Neuroimage 146, 367–375.
Peer, M., Nitzan, M., Bick, A.S., Levin, N., Arzy, S., 2017. Evidence for functional networks within the human Brain's white matter. J. Neurosci. 37 (27), 6394–6407.
Pettersson-Yeo, W., et al., 2014. An empirical comparison of different approaches for combining multimodal neuroimaging data with support vector machine. Front. Neurosci. 8.
Phelps, E.A., Sharot, T., 2008. How (and why) emotion enhances the subjective sense of recollection. Curr. Dir. Psychol. Sci. 17 (2), 147–152.
Poldrack, R.A., 2019. Predictive Models Avoid Excessive Reductionism in Cognitive Neuroimaging. pp. 1–6.
Poldrack, R.A., Mumford, J.A., 2009. Independence in ROI analysis: where is the voodoo? Soc. Cogn. Affect. Neurosci. 4, 208–213.
Poldrack, R.A., et al., 2017a. Scanning the horizon : towards. Nat. Publ. Gr. 18 (2), 115–126.
Poldrack, R.A., et al., 2017b. Scanning the horizon: towards transparent and reproducible neuroimaging research. Nat. Rev. Neurosci. 18, 115–126.
Reislev, N.L., Dyrby, T.B., Siebner, H.R., Kupers, R., Ptito, M., 2016. Simultaneous assessment of white matter changes in microstructure and connectedness in the blind brain. Neural Plast 2016.
Roelofs, J., Muris, P., Huibers, M., Peeters, F., Arntz, A., 2006. On the measurement of rumination: a psychometric evaluation of the ruminative response scale and the rumination on sadness scale in undergraduates. J. Behav. Ther. Exp. Psychiatry 37, 299–313.
Rosenbaum, D., et al., 2017. Aberrant functional connectivity in depression as an index of state and trait rumination. Sci. Rep. 7, 2174.
Sadaghiani, S., D'Esposito, M., 2015. Functional characterization of the cingulo-opercular network in the maintenance of tonic alertness. Cereb. Cortex 25, 2763–2773.
Sampaio-Baptista, C., Johansen-Berg, H., 2017. White matter plasticity in the adult brain. Neuron 96 (6), 1239–1251.
Sarin, S., Abela, J.R.Z., Auerbach, R.P., 2005. The response styles theory of depression: a test of specificity and causal mediation. Cognit. Emot. 19, 751–761.
Schmaling, K.B., Dimidjian, S., Katon, W., Sullivan, M., 2002. Response styles among patients with minor depression and dysthymia in primary care. J. Abnorm. Psychol. 111, 350–356.
Scott, T.A., 2009. Evaluating the Response Styles Theory of Depression Using Descriptive Experience Sampling. UNLV Theses/ Diss. Pap. pp. 124.
Sheehan, D.V., et al., 1998. The mini-international neuropsychiatric interview (M.I.N.I.): the development and validation of a structured diagnostic psychiatric interview for DSM-IV and ICD-10. Journal of Clinical Psychiatry 59, 22–33.
Sheikh, H.I., et al., 2014. Links between white matter microstructure and cortisol reactivity to stress in early childhood: evidence for moderation by parenting. NeuroImage Clin. 6, 77–85.
Sheline, Y.I., et al., 2009. The default mode network and self-referential processes in depression. Proc. Natl. Acad. Sci. U. S. A. 106, 1942–1947.
Shi, Y., et al., 2013. Diffusion tensor imaging-based characterization of brain neurodevelopment in primates. Cereb. Cortex 23, 36–48.
Smith, S.M., 2012. The future of FMRI connectivity. NeuroImage 62, 1257–1266.
Smith, J.M., Alloy, L.B., 2009. A roadmap to rumination: a review of the definition, assessment, and conceptualization of this multifaceted construct. Clin. Psychol. Rev. 29 (2), 116–128.
Smith, S.M., Nichols, T.E., 2009. Threshold-free cluster enhancement: addressing problems of smoothing, threshold dependence and localisation in cluster inference. Neuroimage 44, 83–98.
Smith, S.M., Nichols, T.E., 2018. Statistical challenges in "big data" human neuroimaging. Neuron 97, 263–268.
Smith, S.M., et al., 2006. Tract-based spatial statistics: Voxelwise analysis of multi-subject diffusion data. Neuroimage 31, 1487–1505.
Smith, S.M., et al., 2013. Functional connectomics from resting-state fMRI. Trends Cogn. Sci. 17, 666–682.
Southworth, F., Grafton, B., MacLeod, C., Watkins, E., 2016. Heightened ruminative disposition is associated with impaired attentional disengagement from negative relative to positive information: support for the "impaired disengagement" hypothesis. Cognit. Emot. 9931, 1–13.
Southworth, F., Grafton, B., MacLeod, C., Watkins, E., 2017. Heightened ruminative disposition is associated with impaired attentional disengagement from negative relative to positive information: support for the "impaired disengagement" hypothesis. Cognit. Emot. 31, 422–434.
Spreng, R.N., Stevens, W.D., Chamberlain, J.P., Gilmore, A.W., Schacter, D.L., 2010. Default network activity, coupled with the frontoparietal control network, supports goal-directed cognition. Neuroimage 53 (1), 303–317.
Spreng, R.N., Sepulcre, J., Turner, G.R., Stevens, W.D., Schacter, D.L., 2013. Intrinsic architecture underlying the relations among the default, dorsal attention, and frontoparietal control networks of the human brain. J. Cogn. Neurosci. 25, 74–86.
Steffens, D.C., Taylor, W.D., Denny, K.L., Bergman, S.R., Wang, L., 2011. Structural integrity of the uncinate fasciculus and resting state functional connectivity of the ventral prefrontal cortex in late life depression. PLoS One 6.
Stevens, F.L., Hurley, R.A., Taber, K.H., 2011. Anterior cingulate cortex: unique role in cognition and emotion. J. Neuropsychiatr. Clin. Neurosci. 23, 121–125.
Sui, J., Adali, T., Yu, Q., Chen, J., Calhoun, V.D., 2012. A review of multivariate methods for multimodal fusion of brain imaging data. J. Neurosci. Methods 204 (1), 68–81.
Sui, J., et al., 2014. Combination of FMRI-SMRI-EEG data improves discrimination of schizophrenia patients by ensemble feature selection. 2014 36th Annu. Int. Conf. IEEE Eng. Med. Biol. Soc. EMBC 2014, 3889–3892.
Szucs, D., Ioannidis, J.P.A., 2017. When null hypothesis significance testing is unsuitable for research: a reassessment. Front. Hum. Neurosci. 11, 390.
Tadayonnejad, R., Yang, S., Kumar, A., Ajilore, O., 2014. Multimodal brain connectivity analysis in unmedicated late-life depression. PLoS One 9.
Tao, Y., et al., 2015. The structural connectivity pattern of the default mode network and its association with memory and anxiety. Front. Neuroanat. 9.
Thomas Yeo, B.T., et al., 2011. The organization of the human cerebral cortex estimated by intrinsic functional connectivity. J. Neurophysiol. 106, 1125–1165.
Torgerson, C.M., et al., 2013. DTI tractography and white matter fiber tract characteristics in euthymic bipolar I patients and healthy control subjects. Brain Imaging Behav. 7, 129–139.
Treynor, W., Gonzalez, R., Nolen-Hoeksema, S., 2003. Rumination reconsidered: a psychometric analysis. Cognit. Ther. Res. 27, 247–259.
Ugwu, I.D., Amico, F., Carballedo, A., Fagan, A.J., Frodl, T., 2014. Childhood adversity, depression, age and gender effects on white matter microstructure: a DTI study. Brain Struct. Funct. 220, 1997–2009.
Uludağ, K., Roebroeck, A., 2014. General overview on the merits of multimodal neuroimaging data fusion. NeuroImage 102 (1), 3–10.
Urgerl, Efsun, DeBellis, Michael D., Hooper, Steven R., Donald, P., Woolley, S.C., Provenzale, J.M., 2013. Influence of analysis technique on measurement of diffusion tensor imaging parameters. AJR Am. J. Roentgenol. 200, W510–W517.
Utevsky, A.V., Smith, D.V., Huettel, S.A., 2014. Precuneus is a functional core of the default-mode network. J. Neurosci. 34, 932–940.

van Vugt, M.K., van der Velde, M., 2018. How does rumination impact cognition? A first mechanistic model. Top. Cogn. Sci. 10 (1), 175–191.
Vernooij, M.W., et al., 2007. Fiber density asymmetry of the arcuate fasciculus in relation to functional hemispheric language lateralization in both right- and left-handed healthy subjects: a combined fMRI and DTI study. Neuroimage 35, 1064–1076.
Wang, K., et al., 2015. Individual differences in rumination in healthy and depressive samples: association with brain structure, functional connectivity and depression. Psychol. Med. 45, 2999–3008.
Wang, X., Öngür, D., Auerbach, R.P., Yao, S., 2016. Cognitive vulnerability to major depression: view from the intrinsic network and cross-network interactions. Harv. Rev. Psychiatry 24, 188–201.
Wang, Y., et al., 2017. Resting-state functional connectivity changes within the default mode network and the salience network after antipsychotic treatment in early-phase schizophrenia. Neuropsychiatr. Dis. Treat. 13, 397–406.
Watkins, E., Brown, R.G., 2002. Rumination and executive function in depression: an experimental study. J. Neurol. Neurosurg. Psychiatry 72, 400–402.
Watkins, E., Moulds, M., Mackintosh, B., 2005. Comparisons between rumination and worry in a non-clinical population. Behav. Res. Ther. 43, 1577–1585.
Wells, A., Papageorgiou, C., 2008. Metacognitive therapy for depressive rumination. In: Depressive Rumination: Nature, Theory and Treatment, pp. 259–273.
Westlye, L.T., et al., 2010. Life-span changes of the human brain white matter: diffusion tensor imaging (DTI) and volumetry. Cereb. Cortex 20, 2055–2068.
Williams, A.D., Moulds, M.L., 2007. Investigation of the indulgence cycles hypothesis of suppression on experimentally induced visual intrusions in dysphoria. Behav. Res. Ther. 45 (11), 2780–2788.
Woody, M.L., Gibb, B.E., 2015. Integrating NIMH Research Domain Criteria (RDoC) into depression research. Curr. Opin. Psychol. 4, 6–12.
Wu, X., et al., 2016a. Dysfunction of the cingulo-opercular network in first-episode medication-naive patients with major depressive disorder. J. Affect. Disord. 200, 275–283.
Wu, X., et al., 2016b. A triple network connectivity study of large-scale brain systems in cognitively normal APOE4 carriers. Front. Aging Neurosci. 8.
Yendiki, A., et al., 2011. Automated probabilistic reconstruction of white-matter pathways in health and disease using an atlas of the underlying anatomy. Front. Neuroinform. 5 (23).
Zheng, H., et al., 2015. The altered triple networks interaction in depression under resting state based on graph theory. Biomed. Res. Int. 2015.
Zuo, N., et al., 2012. White matter abnormalities in major depression: a tract-based spatial statistics and rumination study. PLoS One 7.
Züst, M.A., et al., 2015. Hippocampus is place of interaction between unconscious and conscious memories. PLoS One 10.